

UNIVERSITY OF SOUTHAMPTON

CHAIN RUPTURE AS A CONSEQUENCE OF DEFORMATION IN POLYETHYLENE and
FLOW INDUCED ORIENTATION IN A THERMOTROPIC LIQUID CRYSTAL

Thesis submitted in respect of an application for the degree of Master of
Philosophy

Carol Lynn Hammond

September 1984

DEDICATED TO IAN for all his patience and support.

ACKNOWLEDGEMENTS

I wish to express my thanks to the following, for all their help throughout my work, and in the preparation of this report.

Dr. P.J. Hendra, for his supervision and guidance throughout all of my work.

Dr. H.A. Willis and Mrs. V. Zichy (ex I.C.I. Plastics Division) for their helpful discussions.

Mr. S. Jones, Mr. A.J. Peacock and Mr. N. Carthy, for their support and friendship.

Finally, Brenda, Gill and Janette without whose typing this thesis might never have been completed.

UNIVERSITY OF SOUTHAMPTON

ABSTRACT

FACULTY OF SCIENCE

Master of Philosophy

CHAIN RUPTURE AS A CONSEQUENCE OF DEFORMATION, and
FLOW INDUCED ALIGNMENT IN A THERMOTROPIC LIQUID CRYSTAL

by Carol Lynn Hammond

The work reported here covers two areas of study; an investigation into polymeric chain rupture upon deformation and flow induced orientation in a liquid crystal.

Chain rupture upon sample deformation was studied using infra-red spectroscopy, and the polymer used throughout these experiments was polyethylene. Chain rupture was monitored via the new end groups formed upon the broken chain ends in the material, namely carbonyl and terminal vinyl unsaturation. The increases seen in these groups were monitored as a function of deformation under various conditions; sample thickness, atmosphere of drawing, draw ratio, time, and temperature.

Flow induced orientation was investigated in a thermotropic liquid crystal using Raman spectroscopy. Spectral subtractions showed band shifts within the flowing spectra, and these were thought to be indicative of flow induced orientation.

CONTENTS

| <u>CHAPTER 1</u> | | <u>Page number</u> |
|--|--|--------------------|
| 1. INTRODUCTION | | |
| 1.1 Polymeric structure | | 2 |
| 1.2 Polyethylene | | 4 |
| 1.3 Deformation | | 4 |
| a) Theoretical treatments | | 5 |
| b) Experimental Investigation | | 6 |
| (i) ESR | | 6 |
| (ii) Viscosity | | 10 |
| (iii) GPC | | 10 |
| (iv) X-ray Diffraction | | 11 |
| (v) I.R. | | 11 |
| 1.4 Molecular orientation | | 13 |
| 1.4.1 Liquid crystalline phases | | 14 |
| <u>CHAPTER 2</u> | | |
| 2. EXPERIMENTAL METHODS | | 19 |
| 2.1 IR Spectroscopy | | 19 |
| 2.2 Raman spectroscopy | | 20 |
| 2.3 Macromolecular chain rupture | | 21 |
| 2.3.1 IR Spectral assignments | | 22 |
| 2.3.2 Sample preparation | | 24 |
| 2.4 Flowing liquid crystal | | 25 |
| 2.4.1 Spectral assignments | | 26 |
| 2.4.2 Apparatus | | |
| <u>CHAPTER 3</u> | | |
| 3. MACROMOLECULAR CHAIN RUPTURE - RESULTS | | 33 |
| 3.1 Sample thickness | | 34 |
| 3.2 Drawing in oxygen and nitrogen | | 39 |
| 3.3 Draw ratio | | 40 |
| 3.4 Effect of temperature | | 48 |
| 3.5 Chain rupture prior to cold drawing | | 51 |
| 3.6 Quantitative analysis | | 51 |
| 3.7 Two-way drawing | | 53 |
| <u>CHAPTER 4</u> | | |
| 4. INVESTIGATION OF A FLOWING LIQUID CRYSTAL - RESULTS | | 55 |
| 4.1 Shear rate calculation | | 55 |
| 4.2 Results | | 58 |
| 4.2.1 Initial investigation | | 58 |
| 4.2.2 Static and flowing spectra | | 60 |
| 4.2.3 Spectral subtractions | | 60 |
| 4.2.4 Comparison of subtracted spectra of each phase | | 74 |
| <u>CHAPTER 5</u> | | |
| 5. CONCLUSIONS | | 78 |
| 5.1 Chain rupture during deformation | | 78 |
| 5.2 Shear flow alignment | | 82 |
| REFERENCES | | |
| APPENDIX | | |

1. INTRODUCTION

The aims of the work presented in this report were twofold; firstly, it was hoped to establish a standardised method for the monitoring of degradation in polymeric materials using infrared spectroscopy and secondly, to investigate the possibility of flow induced orientation in liquid crystal molecules. Raman spectroscopy was the technique chosen for this latter work. Both of these methods are hopefully going to be brought together in the final stage of an ongoing project, investigating a flowing polymer melt, using infrared spectroscopy.

Both degradation and orientation are of fundamental importance to the polymer processing industry, since they exert a strong influence upon both product quality and service life. It is therefore, relevant to consider the basic processes used within the industry.

Processing behaviour can be related to fundamental polymer properties and the majority of production techniques involve deformation at some stage, as illustrated by the following list of basic processing techniques:-

1. Deformation of a polymer melt - either thermoplastic or thermo-setting, e.g. extrusion, injection-moulding and calendering.
2. Deformation of a polymer in the rubbery state - vacuum forming and pressure forming.
3. Deformation of a solution, either by spreading or extrusion, used in making cast films, synthetic fibres and filaments.
4. Deformation of a suspension, important in the use of rubber latex and PVC pastes.
5. Deformation of low molecular weight polymers, or polymer precursors, as in the preparation of glass-reinforced laminates.
6. Machining operations.

In thermoplastic processing, thermal stability and thermal properties influence melt production. From the preceding list (1) is the most important processing class presently used and therefore flow properties, crystallisation, orientation and shrinkage are all of primary importance. Any details which may come to light as to the effects these parameters may have during processing or on in-service performance are readily sought.

1.1. Polymeric Structure

For most practical purposes, a polymer may be defined as a large molecule built up of repeating small chemical units. In the case of most thermoplastics of which polyethylene is the 'simplest' molecule, there is only one repeat unit involved, and it is basically a long chain of repeating $-(\text{CH}_2)-$ methylene groups;

Chain lengths may vary. However, most commercial polymers consist of 20,000 - 30,000 units. The materials are of very high molecular weight and are hence called macromolecules. In structural comparison with naturally occurring polymers, such as proteins, cellulose and lignin, the synthetic polymers produced by man are relatively simple and of short chain length.

Simple molecules such as water and sodium chloride, can exist in any one of three very distinct states, i.e. solid, liquid or gas. However, in polymers, changes of state are less well defined and may well occur over a finite temperature range, making the investigation of molecular behaviour very interesting. For many years, workers have used several techniques and theories to assess and explain observations seen under certain experimental conditions (1).

Chain flexibility, interchain attraction and the regularity of the polymer as determined by environmental conditions all influence the state of the polymer. The material may behave as a rubber, a glass-like resin, a melt, a hard crystalline solid (below T_g or when a high degree of crystallinity is present) or a flexible crystalline solid (above T_g or in a material with a moderately low degree of crystallinity). Obviously, all of the above mentioned characteristics will influence other physical properties, for example, melt viscosity, yield strength, modulus and impact strength. The melt viscosity, of a polymer at a given temperature is a measure of the rate at which chains can move relative to each other, and is controlled by the chain flexibility and the degree of entanglement. Low flexibility gives highly viscous melts, e.g. PTFE, PVC, as compared to polyethylene and polystyrene, which give relatively low viscosity melts ⁽¹⁾.

Molecular weight has considerable influence on such values for any polymer, as does chain branching and branch length, thereby producing a considerable range of values for any one system. Therefore, all quoted values for a polymer, with regard to its properties must be related to the conditions under which they were obtained.

Mechanical properties such as yield strength and modulus are both greatly affected by intermolecular attraction, molecular weight and the type and amount of crystalline structures present. Whether a material exhibits brittle fracture or appears tough depends on temperature and the strain rate, that is, it is a function of the rate of deformation. In the case of crystalline materials, toughness will depend upon the degree of crystallinity and the size of crystalline structures. Polystyrene, polymethylmethacrylate and UPVC are all considered brittle materials since they break with brittle fracture. Whereas polyethylene and plasticised PVC are considered to be tough.

1.2 Polyethylene

Since the aim of this work was to investigate polymeric degradation as a consequence of deformation, prior to fracture, polyethylene was chosen as the model compound, being a tough, deformable, material with a relatively simple infrared spectrum, therefore facilitating the relatively easy detection of any new chemical groups formed as a consequence of degradation, i.e. chain rupture. In service polymeric components may be deformed inside and outside the elastic limit. In both regions degradation may be accelerated by chain rupture, eventually leading to fatigue failure. The aim of this work was to show that chain rupture may be detected prior to sample failure, and to develop a qualitative and hopefully quantitative means of assessing polymeric degradation.

Since High Density Polyethylene has important industrial applications in mouldings, blown objects and electrical insulation it was considered a worthwhile material to study. However, the intention was to extend the investigation to polypropylene due to its increasing popularity within industry.

Under load polyethylene will deform continuously with time (creep) and will exhibit necking characteristics under the correct applications of strain rate and temperature⁽¹⁾.

1.3 DEFORMATION

To date several theories have been proposed as to the mechanisms active during the deformation of a polymeric material and many experimental techniques have been used to detect evidence of the active processes. In order to substantiate or refute any previous proposals it was necessary to gain an insight into the work so far carried out. However, it should be emphasised here that most previous work has been carried out by stressing samples to fracture.

There are several theories which have been proposed to explain the molecular phenomena occurring during deformation (17-25) and several methods have been used in the evaluation of chain rupture thought to arise as a result of deformation, namely; Electron spin resonance, viscosity measurements, Gel permeation chromatography, X-ray diffraction studies and infra-red spectroscopy (26-33).

a) Theoretical treatments

An in depth explanation of the molecular theories proposed to date is not given here, since the topic is well detailed in the literature. References 17-25 are examples of this material.

On the whole all of the theories put forward explaining the crystalline and amorphous structures present within a semi-crystalline polymer incorporate the phenomena of chain folding, lamellae and amorphous regions. However, several theories exist as to how these structures are made up and combined. When a sample is deformed the molecular arrangements present must obviously undergo some change, and the exact nature and mechanisms active during this process have not yet been proven (17-25).

An important question to be answered is how mechanical loads are transmitted through a material. Macroscopic strength is invariably much lower than that predicted from simple models based upon atomic bond strengths, implying that strength is influenced by the intricacies of structure and imperfections. Strength is a complex function of primary and secondary bonding, inter- and intra-molecular interaction such as crystallinity and entanglements, molecular orientations, and possibly factors as yet unrecognised.

The main reason for the lack of mechanistic identification to date has been due to the difficulty in relating experimental techniques to atomic occurrences (32). Recently modern analytical techniques have been used for this purpose.

To date theories of molecular orientation and deformation⁽¹⁷⁻²⁵⁾ make very little mention of chain rupture, which we feel may be a fundamental component, active during the deformation of a polymeric sample. The following subsections will review the methods used by several workers whilst attempting to substantiate this fact.

b) Experimental investigation of chain rupture during deformation

i) Electron spin resonance

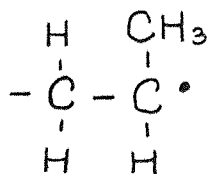
This has been the most extensively used method to date since two free radicals may be expected to result from the homolytic scission of a polymeric covalent bond. If formed in sufficient quantities these radicals should be detectable by ESR.

The most extensive studies have been carried out upon oriented polymer fibres and films, mostly nylon, and results have shown that:

- a) The thermal motion of atomic bonds is a fundamental process in fracture⁽²⁶⁻³¹⁾.
- b) An increase in load tends to bias the thermal motion in favour of bond scission⁽³⁴⁾.
- c) The variation of 'local' stress on the load carrying chains is important⁽³²⁻³⁵⁾.

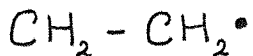
A major disadvantage in the use of ESR to study polymeric fracture is that most polymeric radicals are inherently unstable, having a very high affinity for other unpaired electrons, leading to the loss of radicals⁽³²⁾. The spectrometer will see only the net number of radicals present. Radicals produced by fracture in nylon and by ozone in rubber are fairly stable with a half life of approximately one hour at room temperature. However, other polymeric radicals are very unstable with a half life of one second or less⁽³²⁾. Low temperatures increase radical stability, and are therefore often used, for example:

Sakaguchi and Sohma⁽²⁸⁾ fractured polypropylene samples at 77K, by sawing, and detected the radical



together with peroxide radicals, as other experiments⁽³⁵⁾ had shown.

A ball mill apparatus has also been used by these workers, again at 77K and they identified the primary scission radical for polyethylene as being



produced for a high molecular weight sample⁽²⁷⁾.

Polypropylene, polytetrafluoroethylene, polymethyl methacrylate and polybutadiene have also been investigated in this way and the exact definitions of radicals generated in these polymers may be found in reference 27. At present we are primarily concerned with those results for polyethylene, as this is the polymer used in our work. Since many polymeric radicals are unstable at room temperature a great deal of work has been restricted to low temperatures. However, it is possible to extrapolate from the number of radicals observed to the number produced by fracture with the help of decay kinetics at the temperature used^(36,37,38). Attempts have also been made to stabilise radicals, for example, Ham and Davis suggested the addition of chlorinal and Chaing suggested oxygen, which he has used in studies with PET and polyethylene⁽³⁹⁾.

The radicals observed by ESR are often not the primary but secondary radicals, resulting from radical migration along the polymer chain, or interaction with impurities, mostly oxygen. Sakaguchi and Sohma⁽²⁷⁾ have found that no radicals are formed during the fracture of low molecular weight organic solids, and in this case it is thought that shear stresses are relieved by rupture of intermolecular Van der Waals bonds, with no breaking of covalent bonds. In a polymer however, the large displacements of the molecule induced in macroscopic fracture requires motion of the long chains. They propose that polyethylene molecules with a degree of polymerisation less than about 90, slip past one another without breaking chemical bonds, whereas chain scission occurs in larger molecules⁽²⁷⁾.

Recombination and inhomogeneous stresses are two factors which are of prime importance in the evaluation of chain rupture either by ESR or any other other technique⁽³⁵⁾.

The most successful work to date using ESR spectroscopy has been carried out on highly drawn nylon fibres, due to the relatively high stability of the radicals produced. Samples of other materials are often subjected to grinding⁽²²⁾, abrasion, and radiation⁽²⁹⁾ in order to obtain the maximum number of radicals. Our aim, on the other hand, was to investigate chain rupture during deformation, prior to sample rupture.

As an investigative technique, ESR is very useful. However, in this particular application, it does have its limitations as stated previously, and summarised below:-

1. Most polymeric systems do not suffer enough chain scission during fracture to permit ESR detection.
2. Heterolysis, rather than homolysis, may occur, hence producing few ESR detectable radicals.
3. Radical migration may destroy the correlation between observed radicals and broken bonds, thus undermining the use of ESR in this work.
4. Radical decay, possibly by radical combination, may be too rapid to be accounted for properly, and radical transfer processes in which adjoining chains are broken with no net increase in radicals may also be too rapid, leading to a gross underestimate of chain scission by ESR.
5. ESR is not able to locate the site of bond scission in the molecular structure, e.g. tie chains, microfibril ends, etc., and is of little use in fracture modelling.

ii Viscosity measurements

Macromolecular chain rupture occurring during deformation of semicrystalline polymers has been investigated by measuring the changes in viscosity - average molecular weight. Stoeckel, Blasius and Crist⁽²⁶⁾ have interpreted results as corresponding to chain rupture concentrations of the order of $10^{18}/\text{cm}^3$ in high strength nylon and PET fibres and $10^{16}/\text{cm}^3$ for polypropylene fibres. On the whole, they found bond rupture concentrations about 10 times larger than those obtained from ESR measurements. Using dilute solution viscometric studies on deformed and undeformed polymers, they reported that samples of Nylon 6, Nylon 6,6 and polyethylenterephthalate showed relatively large amounts of bond rupture. These are materials commonly investigated with ESR spectroscopy since they have fairly stable radicals. The results of viscometry and ESR for the above samples were qualitatively comparable, however the viscosity results showed up to 10 times more chain scission to have occurred than was detected by ESR. Veliev et al⁽⁴¹⁾ have reported the formation of 2×10^{19} ruptures/ cm^3 in polyethylene at room temperature, confirmed by a 48% decrease in M_v . Stoeckel did not reproduce these values, however, he does point out that the viscometric technique has ample sensitivity to detect this likely amount of chain rupture.

iii. Gel Permeation Chromatography (GPC)

Since a measurable decrease in molecular weight is expected to be induced by chain rupture, GPC may be a very useful tool. From experiments on drawn nylon, a reduction in the high molecular weight component is apparent, with a drop in M_n from 34,800 to 30,000 having been detected by some workers⁽³⁰⁾. This corresponds to about 3×10^{18} scissions/gm and is in good agreement with ESR work on nylon, reported previously.

GPC provides information as to which chains in the molecular weight distributions are broken and may be very valuable in future model development⁽³⁰⁾.

iv. X-ray Diffraction Studies

In order to gain an insight as to where and how chain scission may be occurring within a sample, this technique has been used to determine the number, size and distribution of microcracks, thought to stem from chain rupture, due to the low mobility of macromolecular chains within a solid sample. Microcracks show that broken bonds are clustered in submicrocavities, located rather uniformly through the stressed material. Cracks are disc shaped and orientated perpendicular to the stress axis, being 100-1000 μm in size⁽³⁰⁾. Zhurkov has used Small Angle X-Ray Scattering (SAXS) to monitor the accumulation of submicrocracks developed during sample deformation and he proposes that they arise as a result of the coalescence of molecular scissions since macromolecules in solid polymers have low mobility⁽⁴²⁾.

v. Infrared Spectroscopy

Chain scission in polymers may result in the formation of new end groups detectable by IR spectroscopy, a technique only recently used to study mechanical degradation during fracture, even though it is not a new tool in end group analysis⁽³⁰⁾.

The chemical species likely to arise from chain scission and radical formation are methyl, carbonyl and vinyl species. Spectral subtraction of a strained and unstrained sample may be used to give a measurement of the increase in concentration of these groups.



Zhurkov et al (18) have detected these species upon the deformation of polyethylene in air. Samples were fractured under uniaxial tension and the intensities of the bands at 910, 965, 1379 and 1735cm^{-1} increased (see Table 1 for assignments). $9.9 \times 10^{18} \text{cm}^{-3}$ bonds have been calculated as being broken from some results obtained for polyethylene (42).

A chain reaction has been proposed as being initiated by the first homolytic bond scission, producing more end groups than corresponds to the radicals detected by ESR. According to such studies the net number of broken bonds is proportional to, but much larger than, the number of radicals determined by ESR (30).

IR has a significant advantage over ESR in that the end groups once formed should be comparatively stable, facilitating investigations of materials not possible in ESR spectroscopy. Long term creep, fatigue, ageing and longer time scale experiments may also be carried out, using this technique, but are not possible using ESR.

Stresses in polymeric bonds have been shown to produce a slight but measurable shift in the IR absorption frequencies, making it possible to investigate the differential bond loading experienced throughout a sample. It has also been found that films undergo less bond scission than fibres, due to their less fully developed fibrillar structure (40, 43, 44).

In comparison with ESR and viscosity measurements, infrared spectroscopy has detected the concentration of ruptured bonds to be 100-1000 times higher and a chain reaction has been proposed in explanation (42). Polypropylene and polyethylene show relatively little chain rupture as detected by ESR spectroscopy. However, IR has detected a concentration of new end groups of between $4 - 80 \times 10^{18}/\text{cm}^3$, equivalent to $2 - 40 \times 10^{18}$ ruptures/ cm^3 (26).

Having reviewed the techniques used to date in the investigation of chain rupture, it was concluded that infra-red spectroscopy would be the best method to be used in the work to be reported here. It uses stable entities as a means of assessment, was readily available in both a double beam and FTIR mode, and facilitated long term, non-destructive, studies of samples not possible with the other instruments discussed.

It is apparent that most work to date has been done by rupturing highly oriented polymers. However, we chose to investigate chain rupture processes active prior to fracture, during the deformation of previously unorientated samples. This is thought to be a new approach to this system, and it is hoped that the techniques and findings, to be reported in subsequent sections, will provide a useful basis for further development of a non-destructive technique for analysing intact polymeric components during service. This may be of prime importance to industry since it will facilitate the optimising of product design, indicating those areas where components may undergo a great deal of stress and hence fail. It may therefore be possible to improve product design to increase service life.

1.4 MOLECULAR ORIENTATION

As described earlier, the industrial processing of almost all polymers for all applications involves the extrusion of a hot melt. It is therefore very important that we have as full an understanding of the polymeric melt as possible. As yet, little spectroscopic work has been carried out to investigate this phase, and therefore the aim of the polymer group at Southampton University is to investigate polymeric melts using spectroscopic techniques.

Infrared and Raman spectroscopy are both non-destructive highly sensitive methods, capable of indicating orientation, degradation and the crystalline structures present in the system under investigation.

This particular section of the work is concerned with the detection of phenomena exhibited in spectra, which may be conducive of molecular orientation, namely band shifts and possibly changes in relative intensities.

Obviously, the ultimate aim of the group is to directly examine a flowing polymer melt, a point currently being pursued. However, the work reported here was the preliminary investigation into the possibilities of detecting flow induced alignment, and therefore a simpler but representative model was used, namely a liquid crystal, the exact details of which are given in Chapter 3.

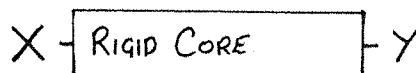
Using a liquid crystal offered a twofold advantage; the molecules being fairly large, rod-like, units may show characteristics indicative of a polymer melt and, secondly, they offer an interesting system for investigation in their own right, due to the thermal phase transitions they undergo. The possible effects of shear on these different forms are of interest. A further point in favour of using a liquid crystal as a model is that many polymeric melts exhibit a liquid crystalline phase under certain specific, yet not atypical, conditions.

1.4.1 Liquid Crystalline Phases

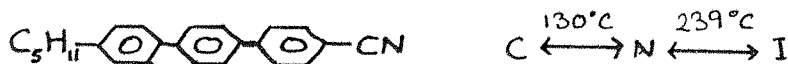
Using a liquid crystal to investigate flow induced orientation provides two avenues of interest; the obvious hope being to detect spectroscopic evidence of shear induced alignment, but also the opportunity arises to investigate the effects of shear upon the separate phases of a liquid crystal.

The following section aims to give an insight into the fundamental properties and differences between the liquid crystalline phases present in the sample chosen, namely the smectic and nematic phases.

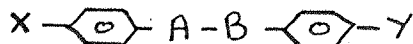
The basic molecular structure required for liquid crystallinity is a 'rigid core' with terminal substituents, i.e.



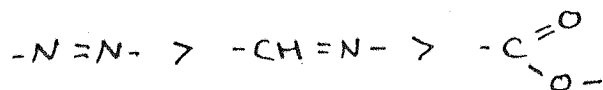
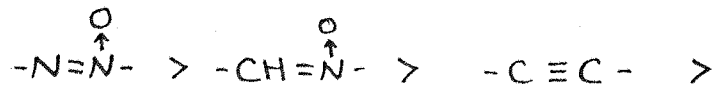
Phenyl groups usually provide the 'core' material and the greater the extent of the core the higher the temperature of the liquid crystal - isotropic transition.



Many mesogens have the structure;



and the following species of $-A-B-$ are arranged in a decreasing order of their ability to induce liquid crystal formation.



This sequence may be rationalised in terms of conjugation linearity and planarity of the rings. However, these generalisations are not strictly enforced in practice and hence liquid crystalline phases and temperatures of transition cannot be predicted precisely on the basis of reasoning offered above.

Liquid crystals are so called because of their apparent intermediate position between the two previously, well defined, extremes of a liquid and a crystal. They have relatively low viscosities but have partial spatial and orientational order.

There are three types of liquid crystal;

- 1) Thermotropics - pure compounds which go through liquid crystalline phases due to changes in temperature.
- 2) Lyotropics - mixtures in which no single component is a liquid crystal. They often involve solutions in water and always have a liquid-liquid interface, e.g. soaps, membranes.
- 3) Chiral Phases - in which the liquid crystal phase has a much greater rotatory power than the original crystal.

The liquid crystal used throughout the experiments to be reported, was of a thermotropic type. The phases and transition temperatures being;

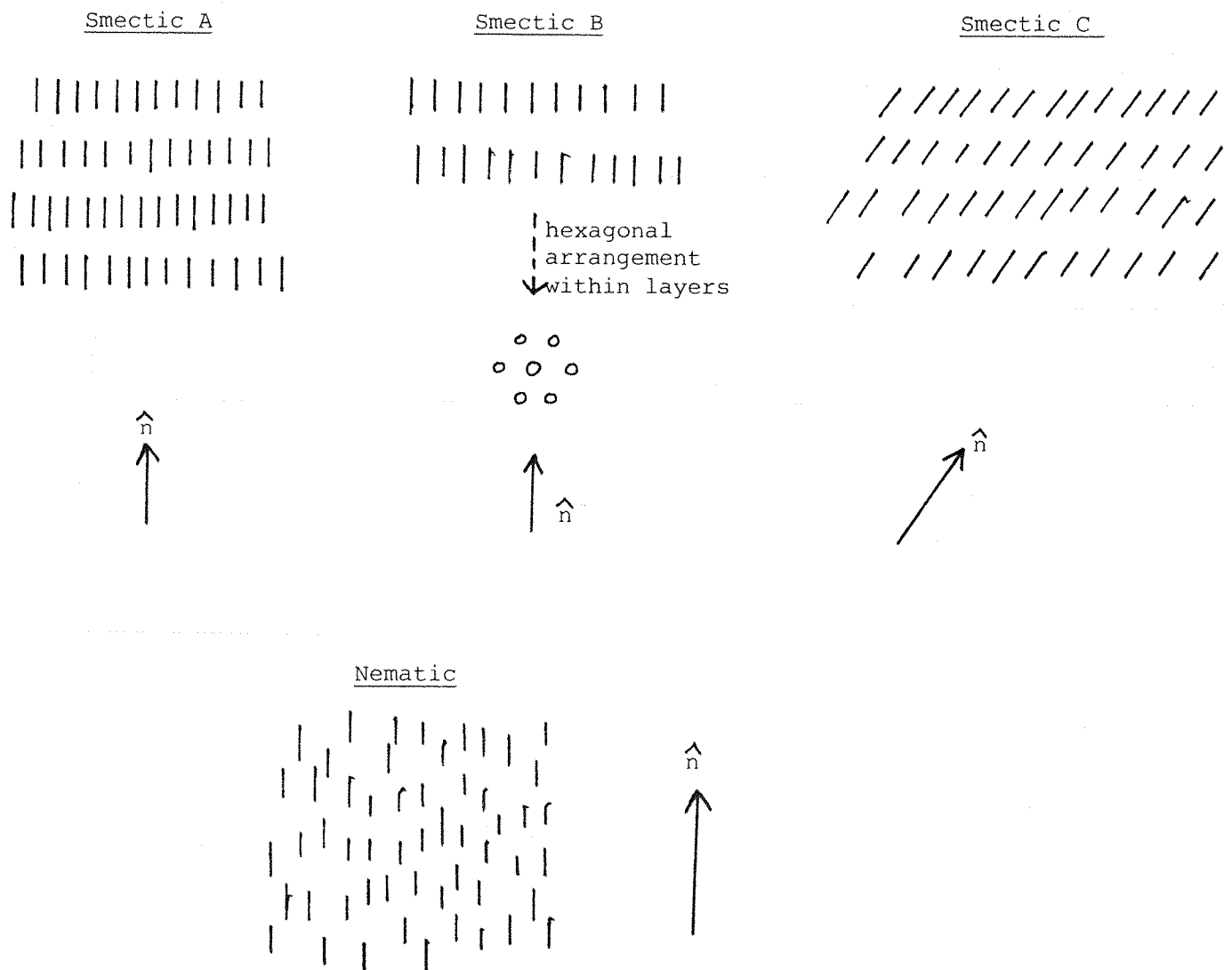
21.5°C 33°C 44.5°C
Crystalline \longrightarrow Smectic \longrightarrow Nematic \longrightarrow Isotropic

Figure 1 illustrates the molecular orientations present in different phases.

The order within a liquid crystalline phase is described by a 'director', 'n', which indicates the preferred direction of a group of molecules, (in other words, the director indicates the average direction in which molecules tend to point).

FIGURE 1

MOLECULAR ARRANGEMENTS WITHIN LIQUID CRYSTAL PHASES



\hat{n} = Director

As can be seen from Figure 1, the smectic phase maintains a little of the spatial order present in the preceding crystalline phase. Molecules tend to exhibit a type of layered structure in which the molecules lie perpendicular to the layer. However, the layers are not perfectly regular and there is incomplete spatial order. There is only short range order in a layer and several forms of the smectic phase exist, called the A, B, C, etc., where the molecules exhibit slight variation in the arrangements within layers. For example, layers may be tilted at an angle to the perpendicular, (Smectic C) or molecules may be arranged hexagonally within a layer, (Smectic B).

In comparison to the smetic phase the nematic is uniaxial, having short range order with respect to the centres of mass, and long range order with respect to orientation.

All definitions and theoretical considerations to date assume that the molecules are cylindrically symmetric, and phases are often described in terms of their order parameters, where a value of one indicates perfect order, and zero complete disorder.

Order parameters have been calculated for various crystals using results obtained from techniques such as refractive index, dielectric constants, diamagnetic susceptibility and more recently spin-spin di-polar coupling in NMR or ESR studies. A precise practical or mathematical explanation of these methods is not warranted here, but several texts may be consulted if such derivations are required⁽¹¹⁻¹³⁾.

It has been found that both magnetic and electric fields induce preferential orientation within a liquid crystalline phase, the exact orientation between the director and direction of the applied field depending upon both the magnetic susceptibility and dielectric permittivity of the molecules in question^(14,16).

If an ionic material is incorporated into certain systems, these species tend to move through the liquid crystal upon the application of an electric field, and will induce alignment in the liquid crystal. Therefore, liquid crystals will exhibit preferential orientation related to the environment in which they exist, and it was hoped that spectroscopic evidence of flow induced alignment would be seen⁽¹⁶⁾.

The vast majority of the work carried out on liquid crystals has been either theoretical, via computer simulation and mathematical interpretation, as shown in the papers by Helfrich , Prost , Lei , Chandrasekhar and Kobayashi⁽³⁻⁷⁾, or practical work which has been carried out upon static systems. For example, Bulkin and Prochaska used Raman spectroscopy to investigate the phases exhibited by p-Azoxyanisole⁽⁸⁾, and Prasad and Venugopalan used both Raman and infra-red in their investigation of orientation in the phases of 80CB⁽⁹⁾. All the work mentioned above was carried out on samples of static liquid crystals. The work to be reported in this thesis, however, uses a flowing liquid crystal, and attempts to illustrate the effects of capillary flow upon molecular orientation as detected by Raman spectroscopy. The limited amount of work which has been carried out by other workers upon flowing liquid crystals and induced orientation, has tended to incorporate the use of treated glass surfaces and magnetic or electrical fields to induce orientation⁽¹⁵⁾. None of these mechanisms were used in the work to be reported here and any variations seen between the Raman spectra of a flowing and static sample arise purely through the variations within the system caused by flow.

CHAPTER 2

EXPERIMENTAL METHODS

One of the tools most widely used in the study of polymers is vibrational spectroscopy. The work reported here used both infra red and Raman spectroscopy. Several texts contain comprehensive explanations of the phenomena leading to the production of spectra when using these techniques⁽⁵¹⁾, and may be readily consulted, therefore it is not felt necessary to dwell in great depth on this topic here. However, a brief explanation is thought necessary.

Since the atoms in a molecule are in constant oscillation about an equilibrium point, and a molecule composed of N atoms has $3N - 6$ (or $3N - 5$ for a linear molecule) vibrational degrees of freedom, one might expect the vibrational spectra of polymeric molecules to be of little use and consist of broad diffuse bands caused by the many individual vibrations in close proximity to each other. However this is not so, and the vibrational spectra of polymers are much simpler than expected. A change in the phase relationship between neighbouring CH_2 groups results in a slight change in the frequency of vibration and therefore only vibrations which have the same frequency, i.e. are in phase, or have a specific phase relationship, may be considered as active in this case. For polyethylene chains the active absorptions are those with a phase shift of zero or π .

2.1 Infra red Spectroscopy

Quantum theory states that an oscillator undergoing simple harmonic motion has discrete quantised energy levels. These levels are separated by $h\nu$ (h = Planck's constant, ν = frequency of vibration). If a vibration induces a fluctuating dipole moment in the molecule, then interaction can occur between this oscillating dipole moment and the electric vector of an electromagnetic field of the correct frequency. This results in the absorption of energy by the molecule. Molecular vibrations generally occur in the infra red region of the electromagnetic spectrum. The high degree of symmetry in many polymeric structures means that some of the fundamental modes may be infra red inactive due to the need for a fluctuating dipole before absorption occurs.

2.2 Raman Spectroscopy

When a sample is illuminated with monochromatic light, the main component of the light scattered off that sample will have a frequency identical to the source, this is called Rayleigh scattering. However, very weakly scattered radiation, shifted mainly to the red end of the spectrum, may also be detected. It is this component of the scattering which is used to produce Raman spectra.

In Raman scattering the selection rule is polarisability, α , and the following statement must be satisfied

$$\frac{\partial \alpha}{\partial q} \neq 0$$

q = the vibration co-ordinate which varies with time⁽⁵¹⁾.

An in-depth explanation of this requirement can be found in the literature^(51,52).

Therefore, the different criteria for infra red and Raman activity means that many vibrations not detected by one technique may be seen in the other.

Raman spectroscopy is favoured for studying samples in-situ, studying microinclusions and where temperature and pressure need to be carefully controlled, since the laser beam is usually very narrow and can be focused on specific regions within the sample. The beam will readily pass through glass, perspex and other transparent media. Infra-red, on the other hand, is only transmitted by specific materials such as KBr and NaCl, making the construction of apparatus that much more difficult. It is fairly easy to direct a laser beam onto a sample since it can be readily angled using glass prisms or even optical fibres, whereas an infra-red beam from an instrument must be diverted using several front silvered mirrors and this is much more difficult to arrange.

Therefore, the advantages over infra-red, with regard to sampling, when using Raman spectroscopy are:-

- 1) In many cases no windows or sample sectioning are required.
- 2) Only a minute patch of the sample is illuminated, making it relatively easy to investigate small samples, inhomogeneities or inclusions.
- 3) Since the method operates in the visible region, high optical transmission is available through glass, quartz, sapphire and several optical polymers. As a consequence the window problem is minimal.
- 4) High and low temperatures and high pressures provide no real problem in the design of apparatus, due to the above points⁽⁵⁰⁾.

However, when choosing to use either infra-red or Raman spectroscopy, one must take into consideration not only the design of apparatus but the aim of the work and what it is hoped to detect. Not all absorptions are equally strong in both techniques, due to the different selection rules which apply.

2.3 Macromolecular Chain Rupture

Having evaluated the techniques previously used in the detection and evaluation of macromolecular chain rupture, infra-red spectroscopy was felt to be the most appropriate technique for use in our work.

The infra-red spectrometer used was a Pye-Unican S.P. 2000 double beam instrument which has a wavenumber accuracy of $\pm 1\text{cm}^{-1}$ between 200-1500cm and $\pm 3\text{cm}^{-1}$ between 1500-4000cm $^{-1}$ giving a repeatability of 1 and 3 wavenumbers respectively. The photometric accuracy of the instrument is 1% T, with a repeatability of 0.5%.

In any spectroscopic technique, an important factor to be considered is the signal to noise ratio. This is particularly important here because the absorptions or absorption differences to be detected in this work were not expected to be large. Hence all spectra were run on a relatively slow scan-speed, often using scale expansion. An added complication frequently found in the use of thin film samples, as in our work, is that of interference fringes. This effect produces regularly spaced sinusoidal fluctuations about the normal baseline, often making it impossible to accurately evaluate absorptions. A possible method for reducing this effect is by roughening the sample surface, however, since this would obviously be detrimental to an investigation of this type, any samples giving rise to interference were, by

Spectra were obtained from the SP 2000 instrument at room temperature at a scan speed of 20 min/scan. The instrument was continuously flushed with dry air.

2.3.1 Infra-red Spectral Assignments

Table I gives the chemical groups thought to be of interest in this work, since they may be generated as new end groups as a consequence of macromolecular chain rupture. Two regions chosen as being the most representative, and the easiest to evaluate from the spectra were the carbonyl region between 1680 - 1760 cm^{-1} and vinyl unsaturation occurring between 900 - 1000 cm^{-1} . The methyl and hydroxyl absorbances were not felt to be quite so discernible and were not used.

TABLE 1 Infra-Red Functional Groups

| <u>Functional Group</u> | <u>Wavenumber</u> | <u>Reference</u> |
|-------------------------|-------------------|------------------|
| - OH | 1070 & 3380 | |
| - CH ₃ | 1379 | 42,46 |
| RCH = CH ₂ | 910,990 | 42,44,45,46 |
| C = C | 1640/1642 | 45,46,47 |
| - CH = CHC - | | |
| " | 1685 | 47 |
| O | | |
| RC - OH | | |
| " | 1705/1710 | 46,47 |
| O | | |
| RCR | | |
| " | 1718 | 45,47 |
| O | | |
| RCHO | 1730/1742 | 42,44,45,46,47 |
| RCOCR | | |
| " | 1740/1742 | 47 |
| O | | |
| RCOOR | | |
| " | 1763 | 47 |
| O | | |
| RCOOH | | |
| " | 1785 | 32 |
| O | | |

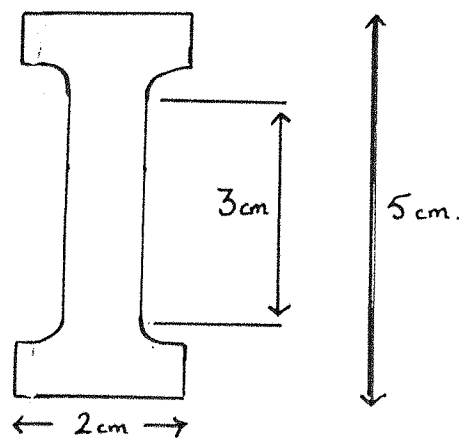
2.3.2 Sample Preparation

The polymer used throughout this set of experiments was a High Density Polyethylene homopolymer, with a melt-flow index of about 0.9g/10 mins and a softening point of 130 - 135°C.

The samples used were in the form of thin isotropic films of uniform thickness, made by pressing pellets of the polymer at 160 - 175°C, initially at 4 atmospheres of pressure to form a melt, then at 50 - 55 atmospheres for 2 - 3 minutes forming a flattened sheet.

The sheets of film produced were cut out to a dumbbell shaped pattern chosen so as to give the sample the correct dimensions for convenient study in the infra-red spectrometer.

Dumbbell shaped test piece



The samples were deformed using a Table Model TM-L slow speed Instron tensometer. The cross-head speed used in all tests was 0.5"/minute. When being drawn in the Instron the samples were aligned as straight as possible within the jaws ensuring that the load was evenly applied throughout the sample.

An insulated box surrounded the jaws and made it possible to provide either an oxygen rich, or an oxygen free, atmosphere for drawing. The latter case was achieved by flushing the box with oxygen free nitrogen. The box could also be heated and cooled.

The specimens were drawn in the Instron to the required draw ratio and then removed from the jaws immediately upon completion, so that the effects of creep would not complicate any findings. An original spectrum of each undrawn sample had to be obtained prior to deformation, thereby facilitating comparison of initial functional group concentration with those of the sample after deformation.

Two regions in the drawn samples were thought to be potentially interesting, namely the neck region and the centre of the drawn region. Spectra were, therefore, obtained at these points upon every sample in case any differences were to be found in end group generation at the two sites.

As mentioned earlier, the carbonyl and vinyl absorptions were thought to offer the most detectable information and, since the carbonyl region includes several possible absorbences which may overlap to give a broader based absorption, total peak area, as opposed to peak height, was used in the evaluation of results obtained, as explained in the Appendix.

2.4 Flowing Liquid Crystal

Raman spectroscopy was chosen as the spectroscopic technique for investigating a flowing liquid crystal for two main reasons:-

- (i) Raman studies of flowing polymer melts are currently underway at Southampton University and therefore some experience had been gained in the use of the technique for this type of work.

(ii) It is possible to use glass for all capillary tubes and reservoirs in the flow apparatus, thereby making manufacture relatively cheap and easy.

2.4.1 Spectral Assignments

The liquid crystal used in this work was K24, a cyano-biphenyl compound, having the structure shown below:



the infra red and raman spectra obtained from a static sample are given in Figure 2 and clearly illustrate the characteristic C ≡ N, and C - H stretching modes, together with absorptions characteristic of phenyl groups.

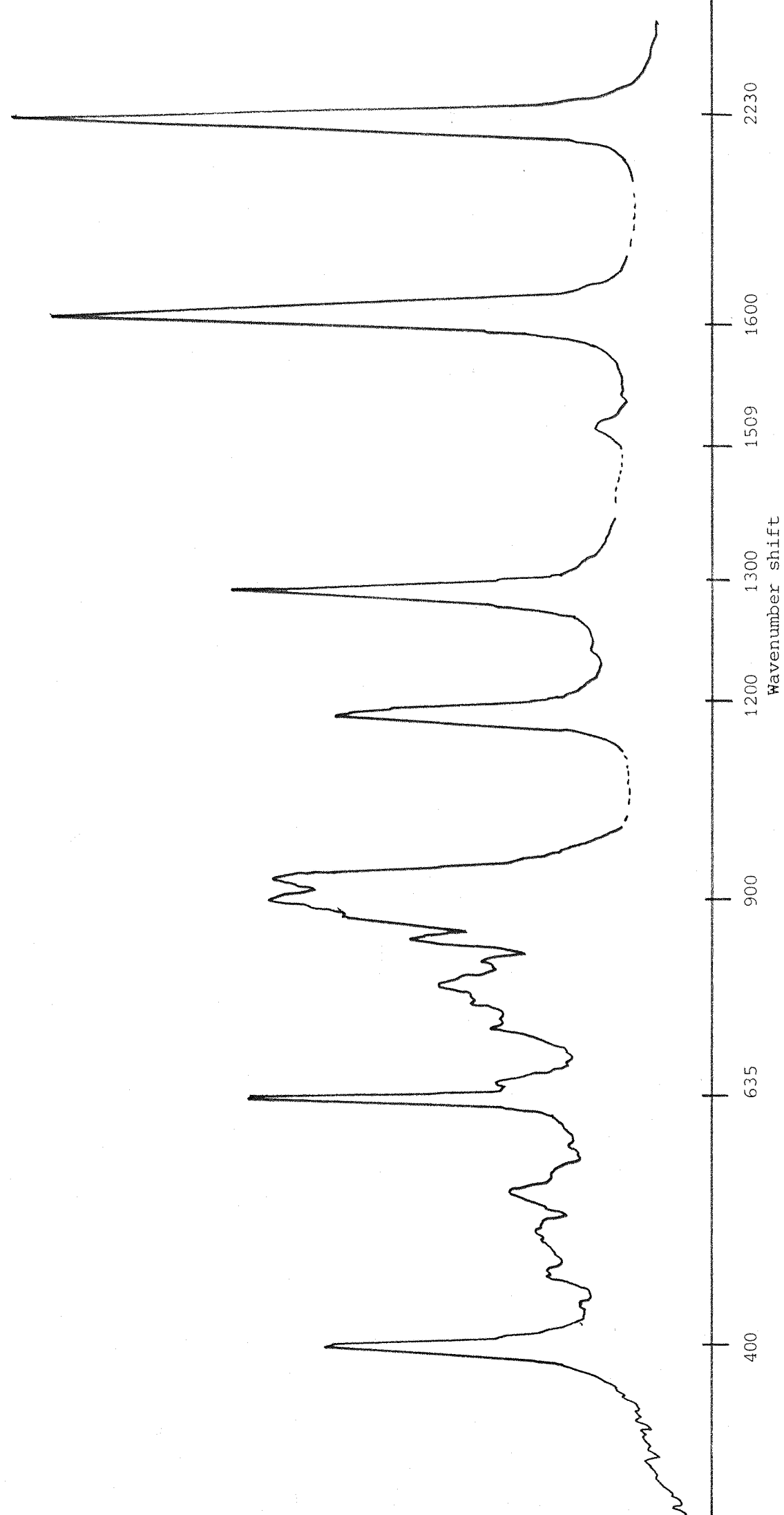
An in-depth normal co-ordinate analysis of absorptions, is not felt to be necessary in this work, however the bands in the raman spectrum thought to be of interest, and their respective assignments, are given below:

TABLE 2 Raman Functional Groups

| <u>Chemical Group</u> | <u>Region in Raman Spectrum (Δ cm⁻¹)</u> |
|--|---|
| -CH stretch | 720 ±10 |
| | 1150 +40 |
| | 1450 ±20 |
| | 2900 |
| Aromatics ring deformation and stretch | 500 - 700 |
| | 1200 |
| | 1600 ±40 |
| | 3100 |
| -C ≡ N stretch | 2250 ±30 |

Figure 2

a) Raman Spectrum of K24



NICOLET MX-1 SAMPLE

2.722

2.130

1.537

0.944

ABSORBANCE

0.352

2600

2300

2000

1700

1400

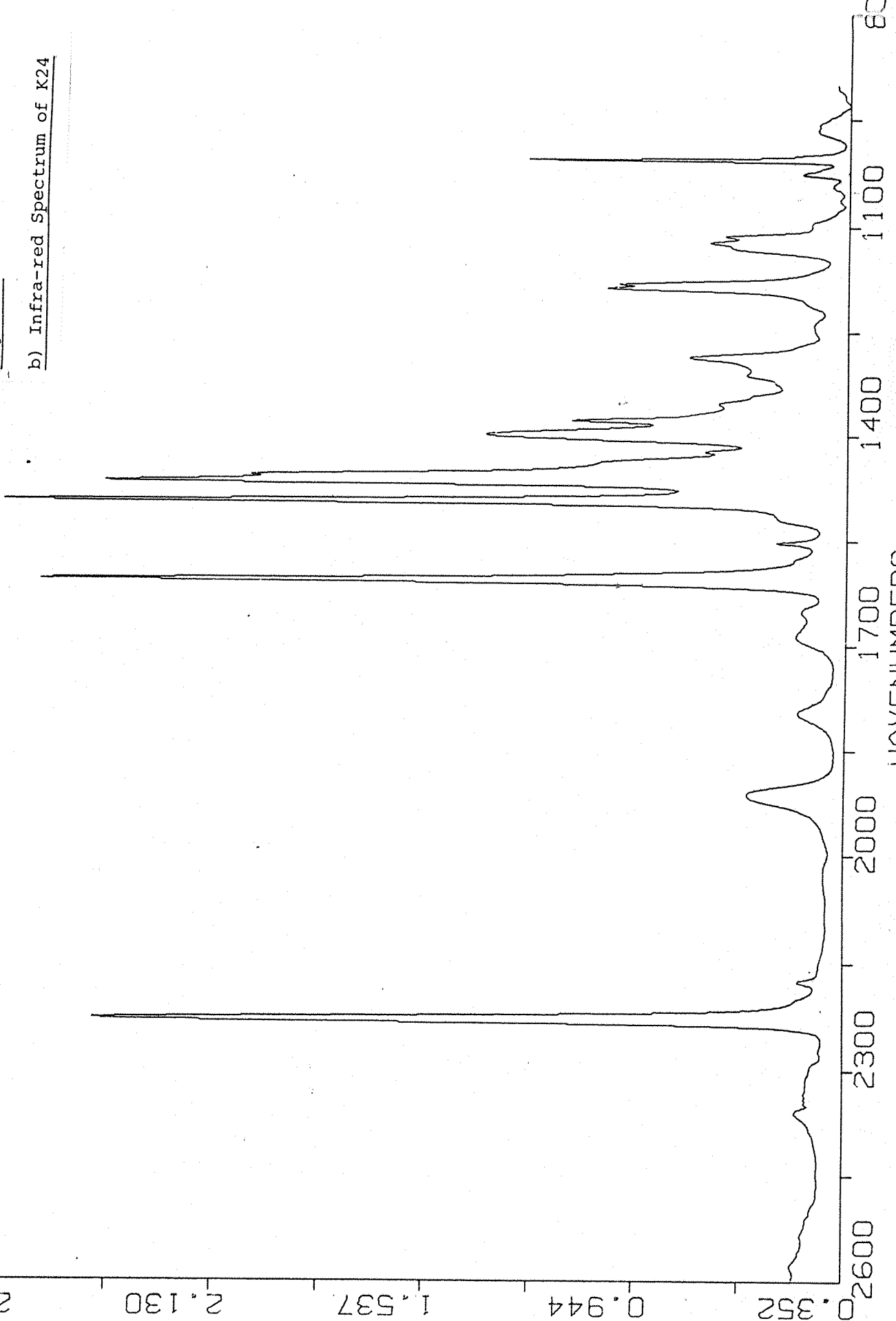
1100

800

WAVENUMBERS

Figure 2

b) Infra-red Spectrum of K24



2.4.2 Apparatus

The main instrument used to obtain spectra was an Anaspec 36, Optical Multichannel Laser Raman Spectrometer. At least 100, 0.1 second, scans were recorded to produce each spectrum, as this was found to provide the optimum signal to noise ratio in the shortest possible time. Spectra were recorded over ranges of approximately 800 wavenumbers, the maximum possible on this machine, and the ranges used were 200 - 1100 cm^{-1} , 900 - 1700 cm^{-1} and 1800 - 2600 cm^{-1} . Spectral subtractions were used in order to evaluate the possible band shifts induced by changes in the flow and shear rate.

Since the Anaspec 36 would not operate below a 200 cm^{-1} shift a Coderg Raman Spectrometer was used in this region.

A thermotropic liquid crystal was used in this work so that all phases could be investigated by providing heat to the sample. The apparatus was therefore insulated and supplied with a heat source. The best means of varying flow rates was found to be by using gas pressure as the mechanism for inducing flow. Nitrogen was used for this, as it is a readily available inert cylinder gas.

Figure 3 shows the apparatus designed and used, based upon the above specifications.

The apparatus consists of two reservoirs for liquid crystal each with a volume of about 5 cm^3 , joined by a capillary tube, with a radius of $3.6 \times 10^{-4} \text{ m}$, and a length of 0.038 m. One reservoir was left empty. The material was then made to flow through the capillary tube, into the adjoining reservoir, under the applied pressure of nitrogen. The inlet of nitrogen was controlled by two electrically operated valves, connected up so that when one valve allowed nitrogen into the apparatus the other was vented to the atmosphere. As the liquid crystal flows out of one side into the other it carries with it a small glass bubble which floated on its surface. There is one glass bubble in each reservoir.

The detectors, labelled A, in Figure 3 are an infra red source and monitor, these were connected to the valve system so that, when the source emission reached the detector the electrical valve was closed, i.e. the nitrogen supply was off and the valve vented to the atmosphere. When the glass bubble interfered with the infra red beam i.e. the detector did not see the source, then the valve opened and the nitrogen flowed into the reservoir therefore pushing the liquid crystal back into the other side under the applied pressure. The arrangement was such that only one valve at a time allowed nitrogen into the system, whilst the other was vented to atmosphere therefore the liquid crystal flowed from one reservoir to the other continually, first in one direction then the other. Raman spectra were recorded of the flowing material in the capillary tube.

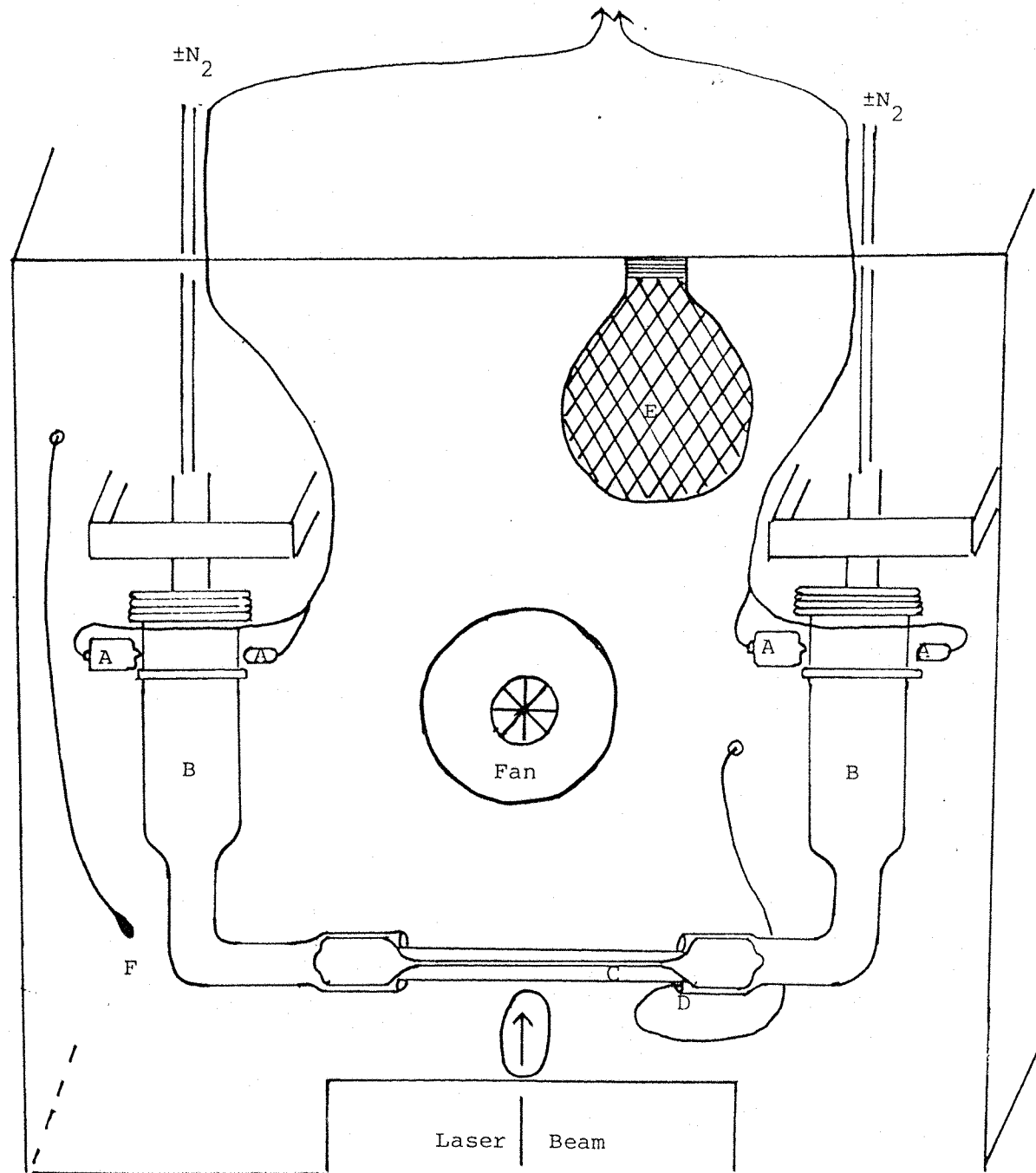
FIGURE 3
Apparatus used for the Investigation
of a Flowing Liquid Crystal

Key

- A = Infra-red source and detector
- B = Liquid crystal reservoir
- C = Capillary tube
- D = Thermocouple
- E = Blackened light bulb, i.e. heat source
- F = Temperature controller thermocouple

This apparatus is contained within an insulated, perspex fronted, sealed box.

To Electrically operated valves



The back and sides of the housing were made of aluminium and held the glassware, fan and heat source in place. The heater used in the box was a blackened 60w light bulb. All of the components, apart from the glassware were painted matt black so that no reflection of the laser beam interfered with the results. The front of the box which faced into the spectrometer was made of perspex therefore facilitating the recording of Raman spectra.

Temperature in the box was monitored by thermocouple, F, which was connected to a temperature controller which switched the light bulb on and off in order to maintain the temperature. Thermocouple D was fastened inside the glassware as close to the liquid crystal as possible, and was used to record the temperature of the material, and provided a means of calibrating the setting of temperature controller with the actual temperature of the material. It was not possible to place a thermocouple directly into the liquid crystal because it would interfere with the flow of material.

The temperature of the box could be monitored to within ± 5 °C, whilst the temperature at the glassware/liquid crystal was measured within ± 1 °C. The stability of a temperature once attained was ± 1 °C

An indication as to the shear rates the liquid crystal was experiencing when it was made to flow at set pressures was obtained from calculations based upon the flow rate, Q and will be explained further in Chapter 4. The temperature of the liquid crystal was noted in order to determine which phase was present.

CHAPTER 3

MACROMOLECULAR CHAIN RUPTURE - RESULTS

At the onset it was necessary to establish whether or not the available instrumentation had sufficient sensitivity to detect the new end groups formed in samples after deformation, and to establish the optimum settings to be used in subsequent runs.

The carbonyl absorptions in polyethylene are likely to be fairly weak and it was important to establish that such absorptions were detectable in prepared samples. The initial exploratory runs all showed small, but detectable, increases in carbonyl absorptions. It was necessary to run all spectra on a slow-scan speed of 20 mins. per scan often with scale expansion, depending upon the intensity of the absorption. All analyses were repeated several times in order to verify the precision of results.

Having established the technique as a potentially useful means of assessing chain rupture, the following variables and their effect upon the extent and type of new end-group generation were assessed:

- i) Sample thickness
- ii) Atmosphere of drawing
- iii) Draw ratio
- iv) Temperature

3.1 Sample Thickness

From the work of Vettegren and Novak⁽⁴⁰⁾ and Roylance with Devries⁽⁴³⁾ in which they state that the distribution of stress amongst chemical bonds is very heterogenous, resulting in some greatly overloaded bonds, it would appear that the original sample thickness might be important. Vettegren⁽⁴⁴⁾ has reported a preferential accumulation of ruptures on the sample surface due, he claims, to a high concentration of overstressed bonds in this area. For his investigation he used an attenuated total reflectance technique in the infra-red. However, we have attempted to establish whether there is indeed a differential component active in chain rupture between the surface and the bulk of the material, using transmission techniques. This method is preferred because it is more generally available, easily operated, rapid and provides unattenuated data on the surfaces and in the bulk, whereas A.T.R. only provides data on the surfaces.

Samples were prepared as described in section 2.3.2 and drawn to a draw ratio of 1 - 2. Films thinner than 100 microns were found to be unsuitable since they tore at the Instron jaws, a point of stress concentration. Appendix I contains a full explanation of how the results were calculated and values are quoted to an accuracy of about 10%.

Table 3 and Figure 4 show that there is a relationship between the increases seen in the carbonyl concentration upon drawing and the original thickness of the sample. Thicker samples show a smaller increase in carbonyl concentration, implying that carbonyl generation is a surface effect possibly due to oxygen availability at the sites of radical generation, or the proposal that a higher concentration of overstressed bonds exists at the surface of the sample, as proposed by Vettegren⁽⁴⁴⁾.

Table 4 and Figure 5 show the relationship between the increases in vinyl unsaturation after drawing and the original film thickness. Again the increase in concentration is smaller for thicker films.

TABLE 3:

CARBONYL INCREASES IN DRAWN FILMS OF DIFFERENT INITIAL THICKNESSES

| Sample thickness μm | Original peak area A (cm ²) | Peak area after drawing B (cm ²) | Difference (B-A) (cm ²) |
|------------------------|--|---|--|
| 60 | zero | 0.15 | 0.15 |
| 80 | 0.23 | 0.34 | 0.11 |
| 85 | 0.08 | 0.16 | 0.08 |
| 85 | 0.05 | 0.30 | 0.25 |
| 95 | 0.05 | 0.33 | 0.29 |
| 105 | 0.05 | 0.24 | 0.18 |
| 110 | 0.07 | 0.25 | 0.18 |
| 160 | <0.05 | 0.80 | 0.04 |
| 160 | 0.05 | 0.30 | 0.25 |
| 200 | 0.06 | 0.25 | 0.18 |
| 220 | 0.05 | 0.15 | 0.19 |
| 220 | 0.05 | 0.13 | 0.09 |
| 225 | <0.05 | 0.07 | 0.03 |
| 300 | 0.05 | 0.21 | 0.16 |
| 390 | zero | 0.05 | 0.05 |
| 410 | 0.1 | 0.1 | zero |
| 415 | 0.1 | 0.2 | 0.1 |
| 530 | 0.1 | 0.11 | zero |
| 570 | <0.05 | 0.15 | 0.10 |
| 780 | 0.06 | 0.06 | zero |
| 800 | 0.08 | 0.07 | zero |
| 805 | 0.06 | 0.07 | zero |
| 820 | <0.05 | 0.08 | 0.04 |
| 820 | 0.06 | 0.1 | 0.04 |
| 830 | 0.04 | 0.05 | zero |

Figure 4

Increase in carbonyl concentration upon deformation against film thickness.

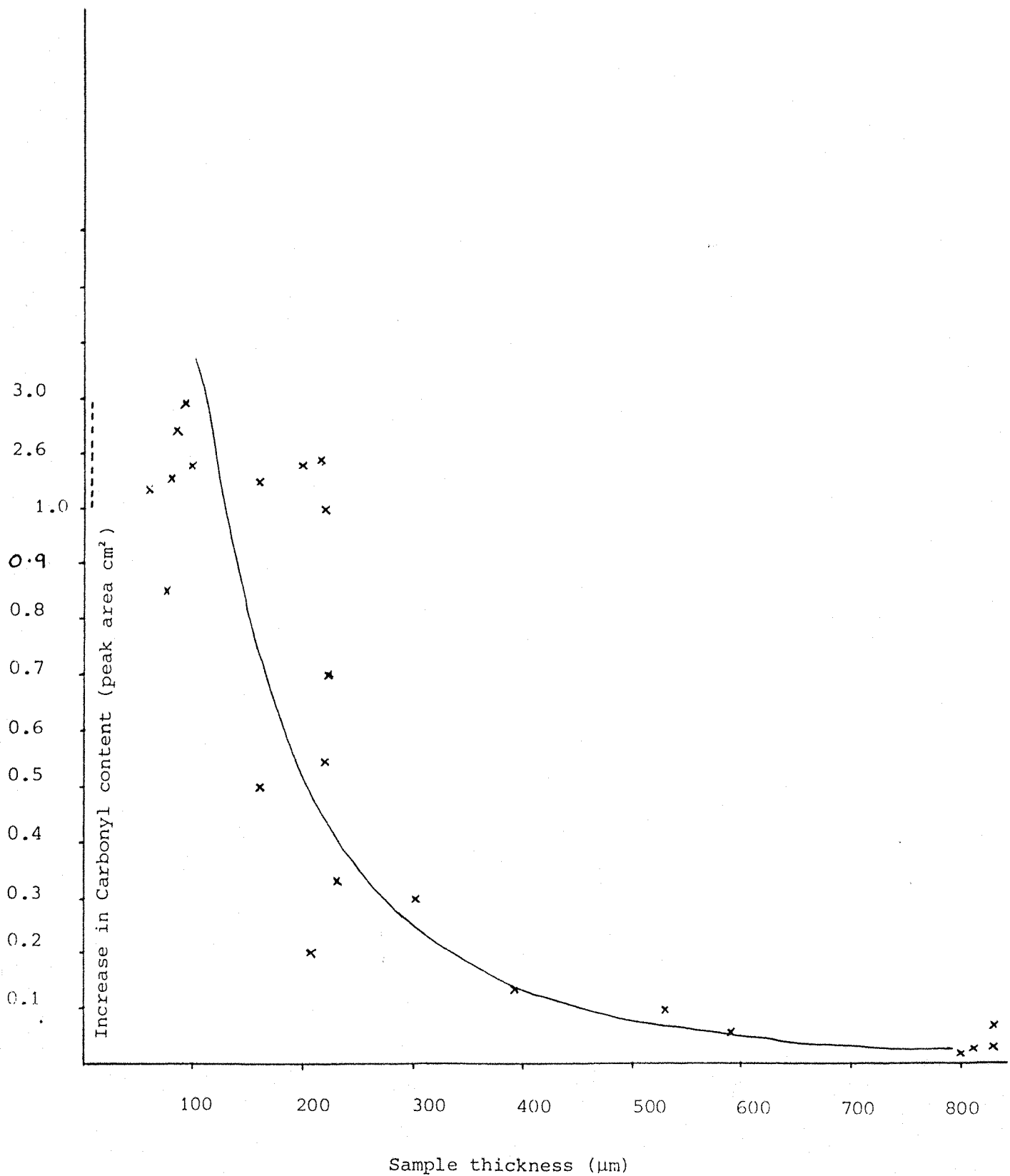


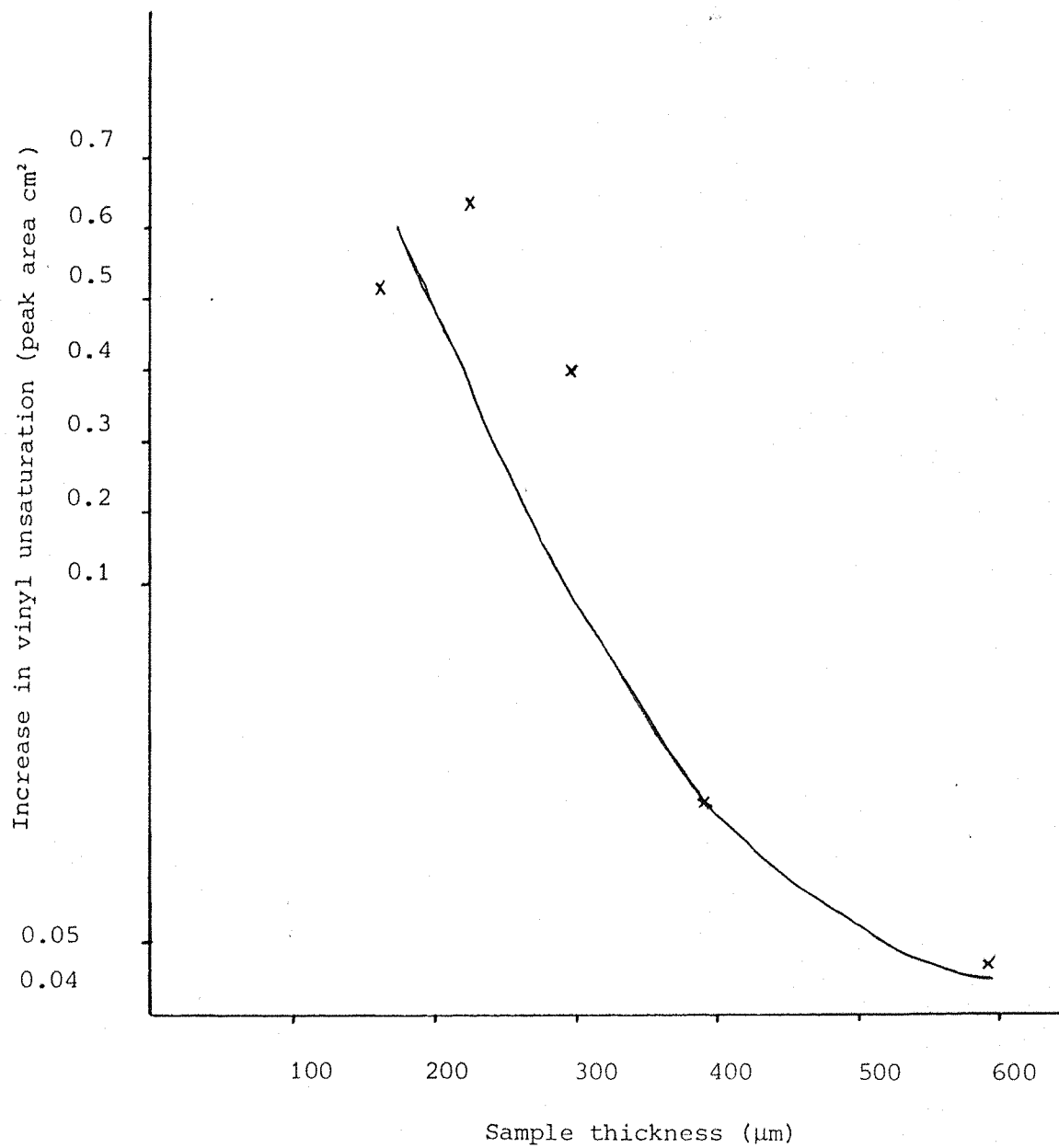
TABLE 4

INCREASES IN TERMINAL VINYL UNSATURATION (990cm) AS A CONSEQUENCE OF DRAWING

| <u>Sample</u> <u>Thickness</u> | <u>Original Peak Area</u> <u>cm²</u> <u>(A)</u> | <u>Peak Area after drawing</u> <u>cm²</u> <u>(B)</u> | <u>Difference (B.A)</u> |
|-----------------------------------|--|---|-------------------------|
| 160 | 0.1 | 0.6 | 0.5 |
| 225 | 0.1 | 0.7 | 0.6 |
| 300 | 0.4 | 0.85 | 0.4 |
| 390 | 0.3 | 0.4 | 0.1 |
| 590 | 0.3 | 0.3 | zero |

Figure 5

Increase in terminal vinyl unsaturation (990 cm^{-1})
against original film thickness.



The two sets of results would appear to substantiate the suggestion that a higher concentration of over stressed bonds, and therefore chain breakages, occurs at the film surface. A potentially important point for product manufacturers and users alike!

3.2 Drawing in Oxygen and Nitrogen

Having detected an increase in the carbonyl and vinyl concentrations as a consequence of sample deformation, further investigation was initiated into the nature of these increases. Firstly, samples were drawn in an atmosphere of either oxygen or nitrogen in order to positively establish that the carbonyl groups seen are a consequence of chain rupture during deformation. The radicals formed by chain rupture will react with molecular oxygen from the surrounding atmosphere.

All the samples were degassed under a vacuum of 0.05 Torr. for one week whilst being exposed to heating and cooling cycles. This was presumed to remove most of the gases present within the samples themselves. Prior to testing, the samples were placed in an atmosphere of the gas in which they were to be tested for 3 - 4 days, thereby allowing the sample to equilibrate within the atmosphere.

Samples were drawn as explained in section 2.3.2 to a draw ratio of 1- 2 at room temperature. After drawing, the samples were left in the atmosphere for up to 4 days to allow any ongoing reactions to reach completion.

It can be seen from the results presented in Table 5 that the increase in carbonyl absorbance is dependent upon the availability of atmospheric oxygen. Samples drawn in an atmosphere of nitrogen show no increase in carbonyl groups, whereas samples drawn in oxygen do show an increase.

Table 6 shows the detected increases in terminal vinyl unsaturation after drawing in either an oxygen or nitrogen atmosphere. There is a difference between the two sets of results, with the concentration of vinyl groups in nitrogen being higher than that formed in an oxygen atmosphere. This would imply that there is some competition between the two reactions leading to the formation of either a carbonyl or vinyl end group.

3.3 Draw Ratio

An initial test investigating the effect of draw ratio upon end group generation indicated a tentative relationship between the two parameters, as can be seen from the table and graph of results (Table 7 and Figure 6). All of the samples used were of a similar thickness $200 \mu\text{m} \pm 30$, so that the effects of the extent of drawing could be evaluated independently of sample thickness.

The encouraging results from this first series of data led to a fuller investigation of this effect, and as in the evaluation of all results reported here several repeat scans were carried out on each sample in order to verify their precision. Since repeats obviously took some time, scans were often repeated a few days apart, and it became apparent that there was a time dependence within the reaction induced by drawing. The set of samples prepared for the investigation of the effect of draw ratio were therefore also used to establish the relationship of end group concentration with time after drawing. Spectra were recorded every 24 hours until a constant end group concentration was reached. The results of the effect of draw ratio and time are given in Table 8 and Figures 7 and 8.

It can be seen that there is a definite increase in the carbonyl and vinyl content of samples, and that this increase is related to the extent of drawing. A larger increase is seen with a higher draw ratio.

Since these samples were also monitored over a period of 94 hours, it became apparent that the increases in absorption themselves rose over a period of time, reaching fairly stable values after 72-94 hours. These observations would suggest that the reaction initiated by deformation, namely chain rupture, can take up to 94 hours to reach completion. The intermediate species, as yet, have not been identified.

TABLE 5

VARIATIONS IN CARBONYL ABSORBANCES OF POLYETHYLENE AFTER DEFORMATION IN OXYGEN AND NITROGEN ENVIRONMENTS

| Sample Thickness (μm) | Atmosphere of Drawing | A Original Peak Area (cm ²) | B Final Peak Area (cm ²) | Increase (B-A) (cm ²) |
|-----------------------|-----------------------|--|---|-----------------------------------|
| 170 | Nitrogen | 0.16 | 0.16 | |
| 206 | | - | - | No increase |
| 150 | | 0.07 | 0.07 | |
| 195 | | 0.23 | 0.23 | |
| 323 | | 0.24 | 0.24 | |
| 190 | Oxygen | 0.07 | 0.22 | 0.15 |
| 163 | | 0.08 | 0.28 | 0.2 |
| 153 | | 0.1 | 0.26 | 0.155 |
| 141 | | 0.02 | 0.265 | 0.245 |
| 296 | | 0.31 | 0.46 | 0.15 |
| 200 | | 0.13 | 0.24 | 0.105 |
| 75 | | 0.18 | 0.41 | 0.23 |
| 155 | | 0.38 | 0.65 | 0.27 |

TABLE 6

VARIATIONS IN TERMINAL VINYL UNSATURATION AFTER DEFORMATION IN OXYGEN AND NITROGEN RICH ENVIRONMENTS

-42-

| Sample Thickness (μm) | Atmosphere of Drawing | Original Peak Area (cm ²) | | Final peak area (cm ²) | | Increase in absorbence (Final _{909cm⁻¹} - Original _{909cm⁻¹}) |
|-----------------------|-----------------------|---------------------------------------|--------------------------------|------------------------------------|---------------------|---|
| | | 909cm ⁻¹ absorbence | 990cm ⁻¹ absorbence | 909cm ⁻¹ | 990cm ⁻¹ | |
| 132 | Oxygen | 1.74 | 0.28 | 2.75 | 0.6 | 1.0 |
| | | 2.2 | 0.7 | 3.4 | 1.0 | 1.2 |
| | | 2.1 | 0.7 | 2.6 | 0.7 | 0.5 |
| | | 2.7 | 0.9 | 4.0 | 1.3 | 1.3 |
| | | | | Average increase = | | 0.33 |
| 200 | Oxygen | 3.1 | 1.8 | 5.7 | 1.5 | 2.6 |
| | | 2.4 | 0.8 | 4.5 | 1.7 | 2.1 |
| | | 2.6 | 0.6 | 3.7 | 1.3 | 1.1 |
| | | 2.7 | 0.6 | 2.7 | 0.6 | No increase |
| 150 | Oxygen | 3.3 | 1.4 | 6.1 | 2.2 | 2.8 |
| | | 2.5 | 0.8 | 4.2 | 1.4 | 1.7 |
| | | 1.1 | 0.34 | 1.2 | 0.3 | 0.1 |
| | | 2.6 | 0.7 | 3.6 | 0.7 | 1.0 |
| | | | | Average increase = | | 0.34 |
| 195 | Oxygen | 3.1 | 1.8 | 5.7 | 1.5 | 2.6 |
| | | 2.4 | 0.8 | 4.5 | 1.7 | 2.1 |
| | | 2.6 | 0.6 | 3.7 | 1.3 | 1.1 |
| | | 2.7 | 0.6 | 2.7 | 0.6 | No increase |
| 190 | Nitrogen | 3.1 | 1.8 | 5.7 | 1.5 | 2.6 |
| | | 2.4 | 0.8 | 4.5 | 1.7 | 2.1 |
| | | 2.6 | 0.6 | 3.7 | 1.3 | 1.1 |
| | | 2.7 | 0.6 | 2.7 | 0.6 | No increase |
| 163 | Nitrogen | 3.3 | 1.4 | 6.1 | 2.2 | 2.8 |
| | | 2.5 | 0.8 | 4.2 | 1.4 | 1.7 |
| | | 1.1 | 0.34 | 1.2 | 0.3 | 0.1 |
| | | 2.6 | 0.7 | 3.6 | 0.7 | 1.0 |
| | | | | Average increase = | | 0.5 |
| 153 | Nitrogen | 3.1 | 1.8 | 5.7 | 1.5 | 2.6 |
| | | 2.4 | 0.8 | 4.5 | 1.7 | 2.1 |
| | | 2.6 | 0.6 | 3.7 | 1.3 | 1.1 |
| | | 2.7 | 0.6 | 2.7 | 0.6 | No increase |
| 141 | Nitrogen | 3.3 | 1.4 | 6.1 | 2.2 | 2.8 |
| | | 2.5 | 0.8 | 4.2 | 1.4 | 1.7 |
| | | 1.1 | 0.34 | 1.2 | 0.3 | 0.1 |
| | | 2.6 | 0.7 | 3.6 | 0.7 | 1.0 |
| | | | | Average increase = | | 0.5 |
| 295 | Nitrogen | 3.1 | 1.8 | 5.7 | 1.5 | 2.6 |
| | | 2.4 | 0.8 | 4.5 | 1.7 | 2.1 |
| | | 2.6 | 0.6 | 3.7 | 1.3 | 1.1 |
| | | 2.7 | 0.6 | 2.7 | 0.6 | No increase |
| 200 | Nitrogen | 3.3 | 1.4 | 6.1 | 2.2 | 2.8 |
| | | 2.5 | 0.8 | 4.2 | 1.4 | 1.7 |
| | | 1.1 | 0.34 | 1.2 | 0.3 | 0.1 |
| | | 2.6 | 0.7 | 3.6 | 0.7 | 1.0 |
| | | | | Average increase = | | 0.5 |
| 75 | Nitrogen | 3.1 | 1.8 | 5.7 | 1.5 | 2.6 |
| | | 2.4 | 0.8 | 4.5 | 1.7 | 2.1 |
| | | 2.6 | 0.6 | 3.7 | 1.3 | 1.1 |
| | | 2.7 | 0.6 | 2.7 | 0.6 | No increase |
| 155 | Nitrogen | 3.3 | 1.4 | 6.1 | 2.2 | 2.8 |
| | | 2.5 | 0.8 | 4.2 | 1.4 | 1.7 |
| | | 1.1 | 0.34 | 1.2 | 0.3 | 0.1 |
| | | 2.6 | 0.7 | 3.6 | 0.7 | 1.0 |
| | | | | Average increase = | | 0.5 |

TABLE 7

RESULTS OF THE EFFECT OF DRAW-RATIO ON CARBONYL AND VINYL END GROUP ABSORBANCES

Carbonyl Absorbtion

| Draw-ratio | Original Peak Area (cm ²) | Final Peak Area after drawing (cm ²) | Difference (Final-Original) (cm ²) |
|------------|---------------------------------------|--|--|
| 0.3 | 0.245 | 0.32 | 0.08 |
| 1.0 | 0.13 | 0.27 | 0.14 |
| 1.2 | 0.11 | 0.19 | 0.08 |
| 2.0 | 0.28 | 0.61 | 0.33 |
| 3.2 | 0.32 | 0.48 | 0.16 |
| 3.65 | - | 0.21 | 0.21 |

Terminal Vinyl Unsaturation (909 cm⁻¹)

| Draw-ratio | Original Peak Area (cm ²) | Peak area after drawing (cm ²) | Difference (Final-Original) (cm ²) |
|------------|---------------------------------------|--|--|
| 0.3 | 2.61 | 3.06 | 0.45 |
| 0.4 | 2.63 | 5.22 | 2.59 |
| 1.0 | 2.39 | 5.05 | 2.66 |
| 1.2 | 2.34 | 3.52 | 1.18 |
| 2.0 | 0.78 | 6.17 | 3.39 |
| 3.2 | 2.93 | 8.53 | 5.6 |

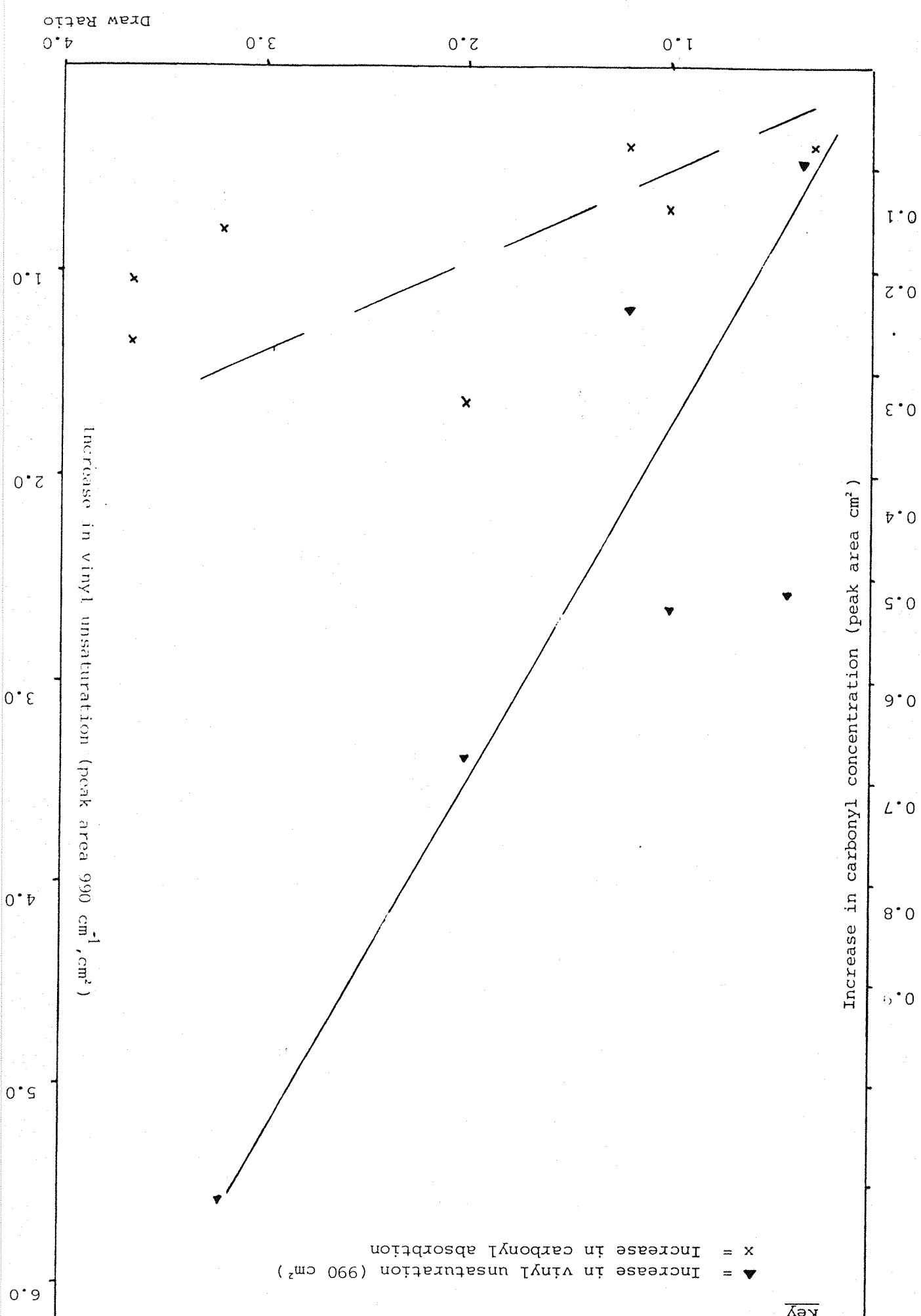


Figure 6

TABLE 8

INCREASE IN CARBONYL ABSORPTIONS WITH DRAW-RATIO, AND TIME AFTER DRAWING

| Draw-ratio | Increases in carbonyl absorption after drawing (cm ²) | | | | |
|------------|---|------|------|------|------|
| | 1 | 2 | 3 | 4 | 5 |
| 0.3 | 0.04 | 0.04 | 0.06 | 0.05 | 0.06 |
| 0.6 | 0.08 | 0.12 | 0.08 | 0.10 | 0.15 |
| 1.35 | 0.14 | 0.14 | 0.14 | 0.17 | 0.17 |
| 2.4 | 0.11 | 0.18 | 0.25 | 0.25 | 0.25 |
| 3.4 | 0.1 | 0.22 | 0.38 | 0.48 | 0.48 |
| 4.6 | 0.14 | 0.27 | 0.61 | 0.78 | 0.78 |
| 5.4 | 0.20 | 0.34 | 0.80 | 0.80 | 1.00 |

KEY

Run 1 = immediately after drawing

2 = after 24 hours

3 = after 48 hours

4 = after 73 hours

5 = after 94 hours.

TABLE 8b

INCREASE IN TERMINAL VINYL UNSATURATION USING 910cm⁻¹ ABSORPTION WITH INCREASED DRAW-RATIO AND TIME

| Draw-ratio | Initial increase in Peak Area (cm ²) | Increase in Peak Area after 72 hours (cm ²) |
|------------|--|---|
| 0.6 | 0.5 | 1.0 |
| 1.4 | 0.7 | 1.46 |
| 2.4 | 1.17 | 1.74 |
| 3.6 | 1.5 | 1.91 |
| 5.4 | 2.25 | 2.52 |

Figure 7

Increase in carbonyl content with Draw ratio and Time

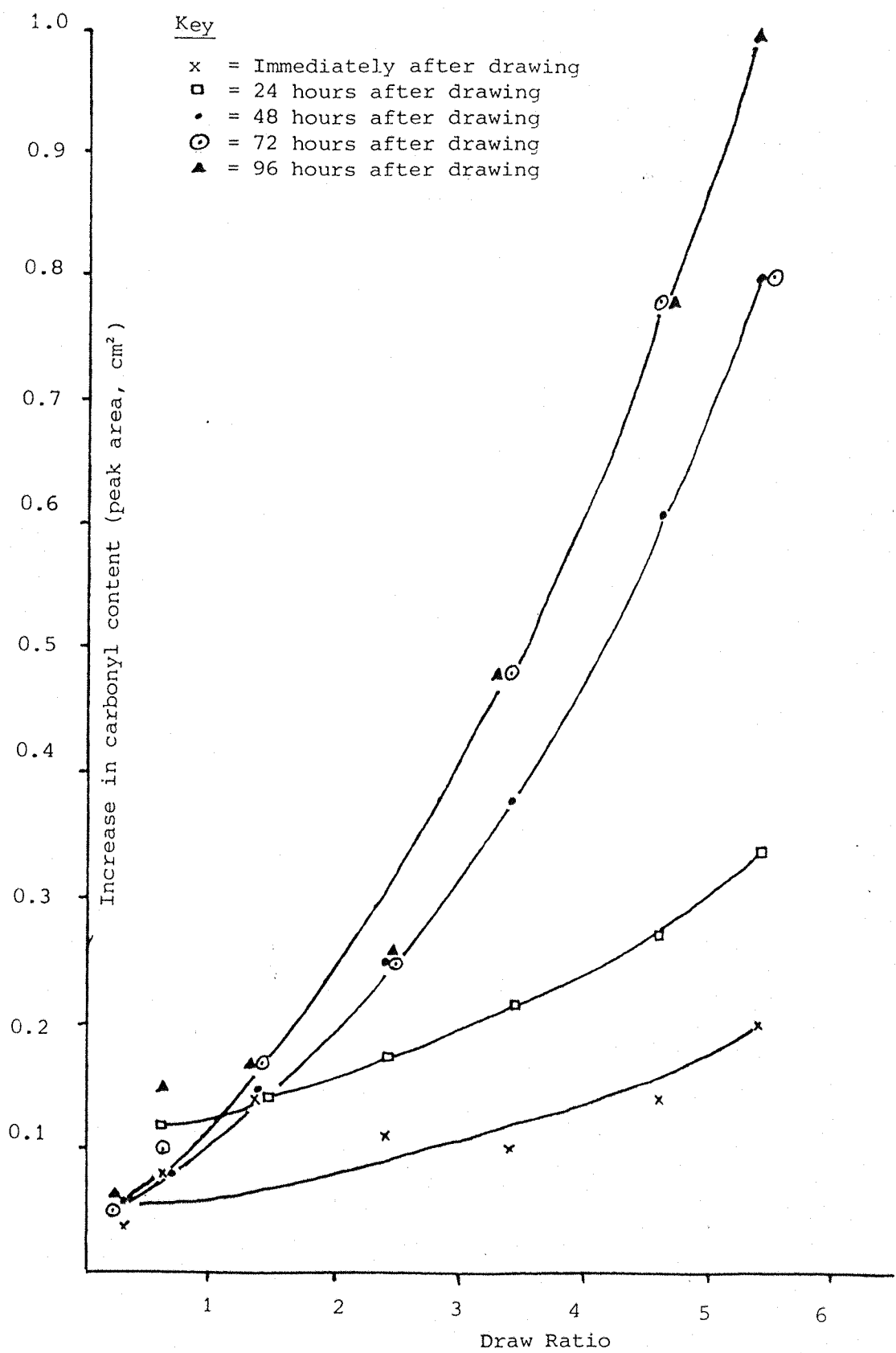
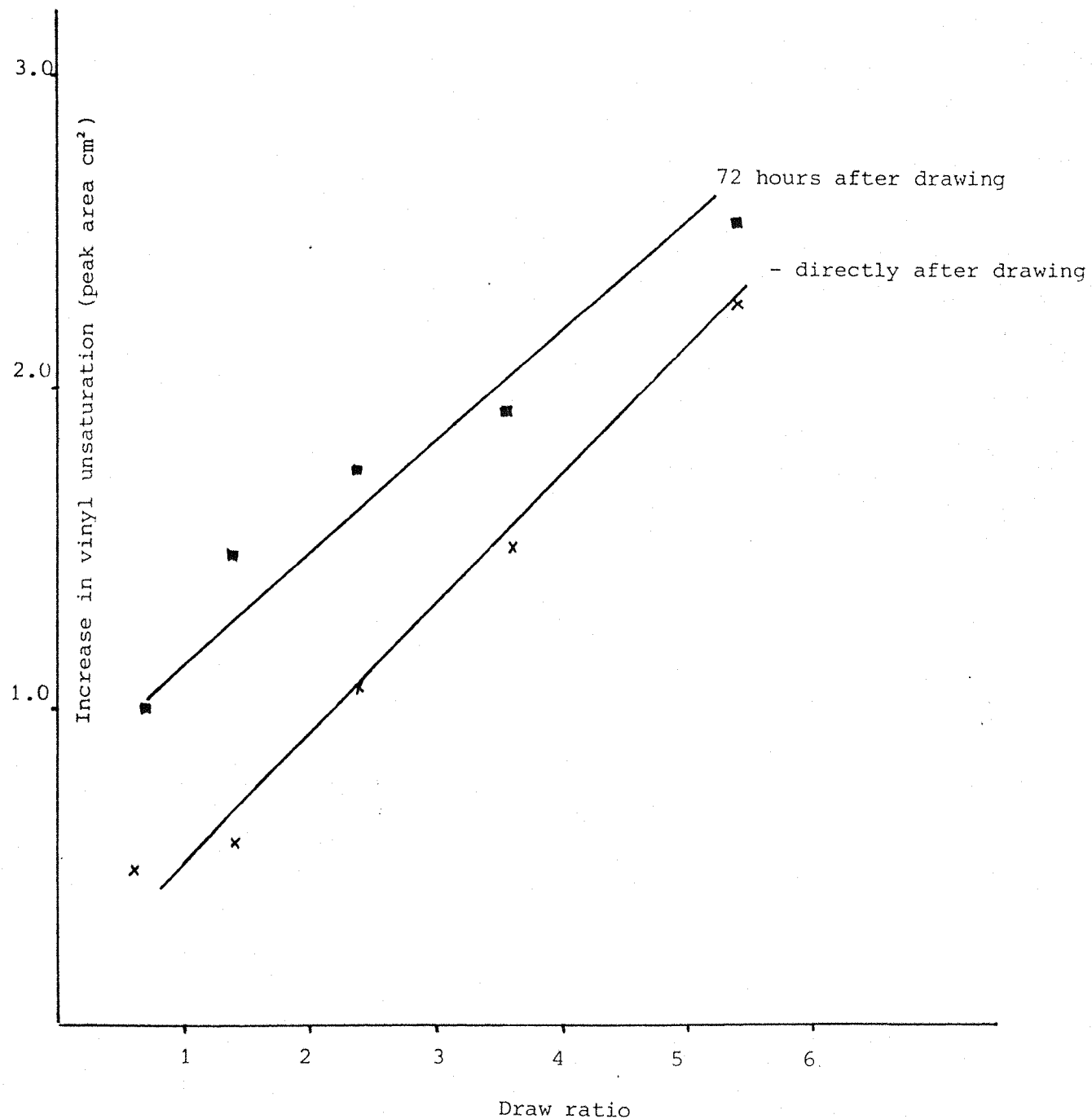


Figure 8

Increase in terminal vinyl unsaturation (910 cm^{-1}) with draw ratio and time



Since these samples were also monitored over a period of 96 hours, it became apparent that the increases in absorption in themselves rose over a period of time, reaching a fairly stable value after 96 hours. This would suggest that the reaction initiated by deformation, namely chain rupture, can take up to 96 hours to reach completion. The intermediate species, as yet, have not been identified.

The results in Table 8 and Figures 7 and 8, showing an increase in end groups absorbance with time, tend to disagree with those reported by Veliev et al (49), who states that no further increase is seen in end group absorbances with time in i.r. analysis up to ten days after deformation.

3.4 The Effects of Temperature

Having evaluated the effect of sample thickness, atmosphere, draw ratio and time, upon end group generation, the final parameter to be looked at during these investigations was temperature. The results are presented in Table and Figure 9.

It can be seen that on the whole the increases in carbonyl and vinyl absorbances become less pronounced as temperature increases. The draw ratio of the specimens is also shown on Figure 9, and increases with temperature. On the whole the results demonstrate that, as the drawing temperature increases, the number of chain breakages decreases. It is possible that this relationship is due to increased thermal energy in the chains facilitating chain slip, rather than rupture, within the material. Had it been possible to achieve high draw ratios at lower temperatures, i.e. below -20°C, one might have expected a great deal of chain rupture, due to the relatively low mobility of chains at these temperatures. Unfortunately at such low temperatures the material is sufficiently brittle to make this test impracticable.

TABLE 9

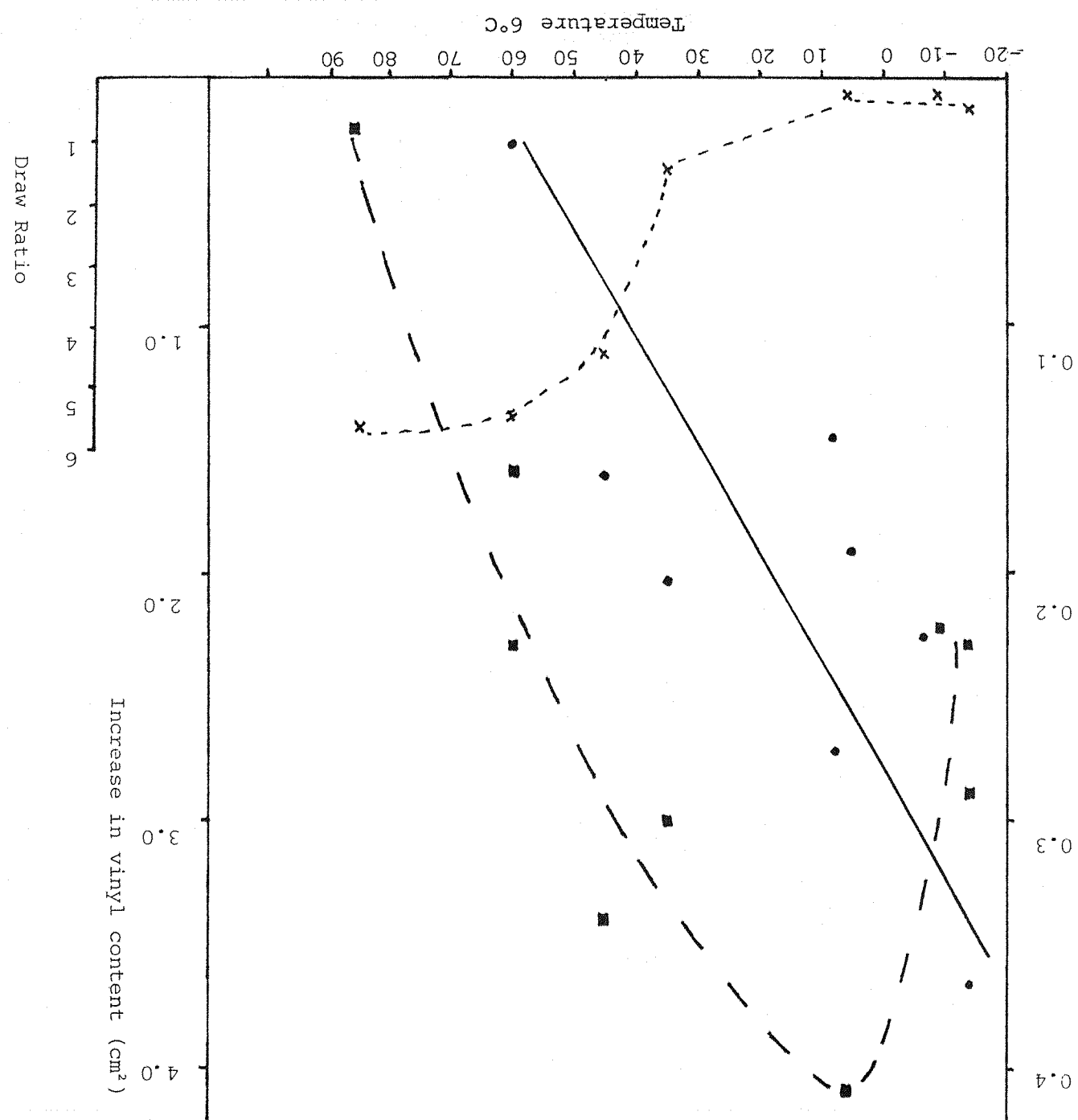
THE EFFECT OF TEMPERATURE ON END GROUP GENERATION

Carbonyl Concentration

| Temperature (°C) | Draw-ratio | Original Peak Area (cm ²) | Peak Area after drawing (cm ²) | Increase (Final-original) (cm ²) |
|------------------|------------|---------------------------------------|--|--|
| -14 | 0.3 | 0.01 | 0.30 | 0.29 |
| -9 | 0.3 | 0.04 | 0.26 | 0.22 |
| 6 | 0.3 | 0.06 | 0.47 | 0.41 |
| 35 | 1.5 | 0.07 | 0.37 | 0.3 |
| 45 | 4.5 | 0.05 | 0.38 | 0.34 |
| 60 | 5.9 | 0.03 | 0.26 | 0.23 |
| 85 | 5.6 | 0.02 | 0.04 | 0.02 |

Vinyl Concentration

| Temperature (°C) | Draw-ratio | Original Peak Area (cm ²) | Peak Area after drawing (cm ²) | Increase (cm ²) |
|------------------|------------|---------------------------------------|--|-----------------------------|
| -14 | 0.3 | 7.67 | 11.36 | 3.69 |
| -9 | 0.3 | 2.7 | 4.94 | 2.24 |
| 6 | 0.3 | 2.95 | 4.89 | 1.94 |
| 35 | 1.5 | 2.56 | 4.59 | 2.03 |
| 45 | 4.5 | 2.84 | 4.45 | 1.61 |
| 60 | 5.5 | 2.42 | 2.68 | 0.26 |



Effect of temperature upon end - group generation

Temperature $^{\circ}\text{C}$

Key

- = Increase in vinyl content
- = Increase in carbonyl content
- = Draw ratio

3.5 Chain Rupture, due to Sample Loading, Prior to Cold Drawing

In order to gain further insight into the effect of stress upon polymeric materials, several samples were stressed just below their yield point and left for 30 minutes, either allowing the load to drop due to the effects of creep or using constant load facilities. The results from these tests were not conclusive, however it was possible to detect small increases in the carbonyl and vinyl concentrations of some samples, indicating that chain rupture under tension occurs long before the sample shows physical signs of deformation.

Those samples subjected to a constant load rather than an initial loading followed by creep tended to show higher increases in carbonyl concentrations than the latter, as would be expected. The actual increases found ranged between 10-20% for the samples exhibiting creep and 15-40% for those under constant loading conditions. However, further work is necessary to verify these findings.

3.6 Quantitative Analysis

Having demonstrated that there is an increase in end group concentration upon deformation, prior to fracture, an attempt was made to quantify these results, using the Beer-Lambert Law. The law states that the amount of radiant energy absorbed or transmitted by a specimen is an exponential function of the concentration of absorbing substance present and the sample path length, (50) i.e.

$$A = \epsilon \cdot c \cdot l$$

where

A = Absorbence

ϵ = Molar absorptivity or extinction coefficient.

c = concentration

l = Path length

Since the absorption and path length (sample thickness) are known for each sample, a value of ϵ is essential, in order to calculate concentration. The carbonyl groups were chosen as the species to be quantified in this analysis and ϵ was estimated using the carbonyl absorption in the spectrum of a known concentration of oleic acid. Extinction coefficients in the i.r. are relatively sensitive to parameters such as; the overall symmetry of the molecule, its environment, solvents and intra-and inter-molecular electrostatic forces. Since the aim here was to derive a value as close to the real one as possible, oleic acid was used since it was ~~an~~ available long chain species containing (CH_2) groups plus a terminal COOH group. A 1mm solution cell was used.

From the calculated value of ϵ and the recorded spectra, carbonyl concentration as $mol\ dm^{-3}$ was calculated. These values were converted to carbonyl groups per cubic centimetre using Avagadros Number. The results are given in Table 10.

TABLE 10

QUANTITATIVE ANALYSIS

Calculated Values for the
Number of Carbonyl Groups
Present (Number/cm³)

Samples from Draw-Ratio Results

| | | |
|--------------|-----|----------------------|
| Draw-ratio = | 1.6 | 4.4×10^{19} |
| | 3.0 | 6.8×10^{19} |
| | 6.0 | 4.7×10^{20} |

Sample Thickness Results (μm)

| | | |
|-------------------|-----|-----------------------|
| Initial thickness | 200 | 1.54×10^{20} |
| | 800 | 2.55×10^{19} |

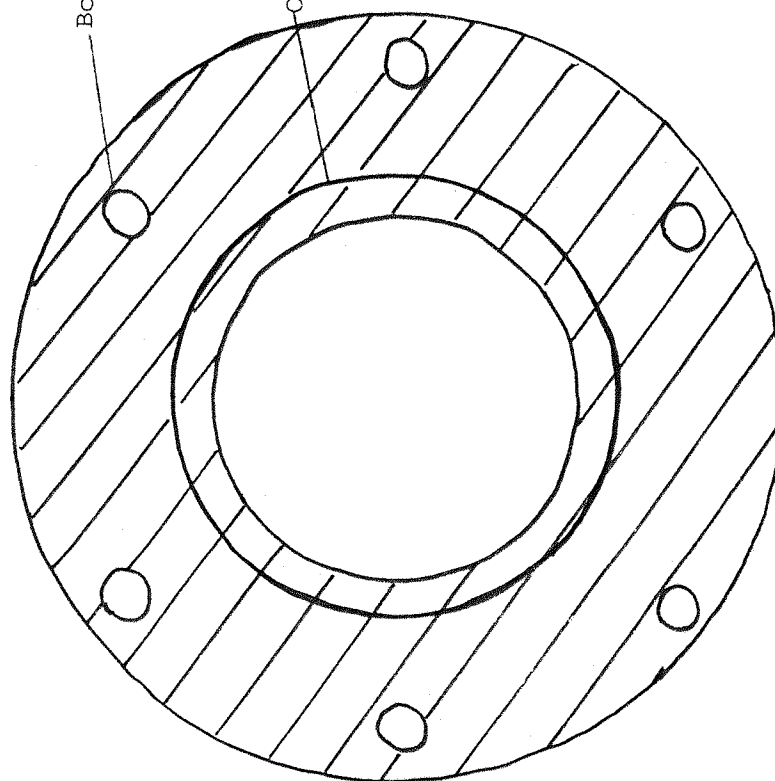
From these results it can be seen that values are close to those reported by other workers for chain ruptures, measured using i.r. viscosity and GPC. Obviously, variations occur between each set of reported values obtained by different workers, since analytical techniques and polymers vary. However, the results in Table 10 do illustrate that the methods reported here may be used in a quantitative manner. Further work refining the quantitation analysis would be of considerable use, since then a reliable method of detecting chain rupture would be available and hence useful in industrial applications.

3.7 Two-Way Drawing

All types of film deformation, such as film blowing and vacuum forming, involve two way deformation and therefore a little work has been done on two-way drawn specimens in an attempt to assess whether chain rupture could be detected. The apparatus shown in Figure 10 was used, in which a small bubble was blown from a sample of the film, by pumping water into the sealed apparatus. Water was used as the pressure medium since a slow controlled increase in pressure could be achieved. It would have been difficult to have such close control over inflation had a gas been used.

To date, it has only been possible to achieve very low draw ratios, i.e. less than 1, at room temperature. Increasing temperature did facilitate higher draw ratios, but as mentioned in 3.4, increasing temperature reduces the amount of chain rupture. The increases in end group concentration detected to date have only been very small, in the order of 10-20% compared to values often in excess of 100% in one way drawing, as reported in an earlier section. Therefore the results of this test are inconclusive and specific values are not quoted at this stage, and the technique of two-way drawing in the laboratory needs to be modified and improve in order to obtain higher draw ratios.

TOP PLATE

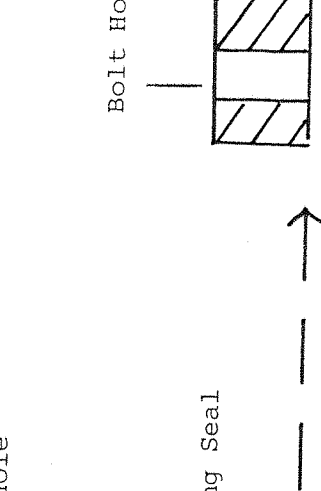
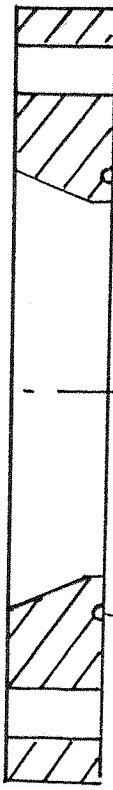


Bolt Hole

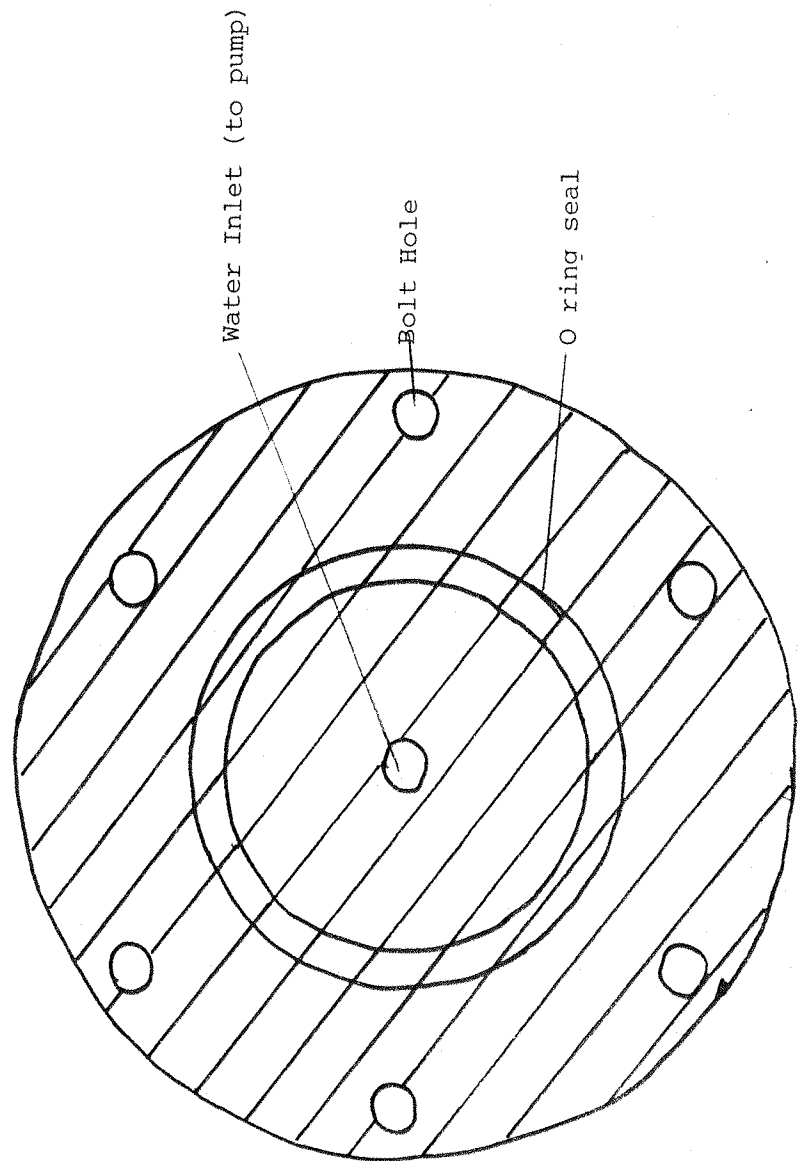
O-ring Seal

Bolt Hole

O ring seal



BOTTOM PLATE



Bolt Hole

O ring seal

Water Inlet (to pump)

Chapter 4

Investigation of a Flowing Liquid Crystal - Results

The apparatus used throughout these experiments is described in Chapter 2, and firstly, in order to relate any changes in the spectrum to shear induced molecular alignment, it was necessary to have an indication of the shear rate of the flowing material.

4.1 Shear Rate Calculation

Since the liquid crystal was flowing through a capillary tube, the equations relating to this type of flow were used⁽⁵³⁾.

$$\text{Shear rate } (\dot{\gamma}) = \frac{4Q}{\pi R^3}$$

P = Pressure

R = Radius of capillary

l = length of capillary

Q = Flow rate

The values calculated using these equations and the settings used throughout experiments are given in Table 11.

$$\text{Shear stress } (\tau) = \frac{PR}{2l}$$

21

$$\text{Apparent viscosity} = \frac{\tau}{\dot{\gamma}}$$

Table 11 Shear Rates

| Gas Pressure (psi)* | Liquid crystal phase | Shear rate (s ⁻¹) | Shear Stress | Apparent viscosity η |
|------------------------|-------------------------|-------------------------------------|-----------------|---------------------------------|
| 30 | Smectic | 1.0 | 1361 | 1361 |
| | Nematic | 1.3 | | 1047 |
| 50 | Smectic | 3.9 | 2270 | 582 |
| | Nematic | 5.2 | | 437 |
| 100 | Smectic | 5.8 | 4540 | (783) |
| | Nematic | 23.0 | | 197 |

* 1000 psi = 6.895 Mega Nm⁻²

From the results in Table 11. it can be seen that the shear rate at any given pressure increases with a change in phase of the sample, from the smectic to the nematic phase. The nematic phase is less viscous than the smectic.

It is also apparent that the viscosity of the sample, in any one phase, on the whole decreases with increased pressure. This type of flow is known as non-newtonian.

Non-newtonian behaviour can arise in a number of ways, but the two most commonly accepted are:

- a) Molecules which are extensively entangled and randomly orientated at rest, under shear become orientated and the entanglement is reduced. At very high shear rates this orientation may be complete and near - Newtonian behaviour will be observed.
- b) Highly solvated molecules, with increasing shear rate may have some of the solvated layers sheared away, leading to a reduction in the apparent viscosity.

In consideration of these two proposals and the structure present in K24, orientation is thought to offer the best explanation for the non-newtonian behaviour of the system.

In the work reported here increased shear rates were achieved by increasing the pressure applied to the system to induce flow. An alternative way of increasing shear rate would have been to reduce the radius of the capillary used, however due to the inconvenience this would have caused in assembling and disassembling of the apparatus between runs, pressure was used to vary shear rate.

4.2 Results

All of the Raman spectra for this work were recorded using the green (5145 Å) emission from Argon laser.

4.2.1 Static and Flowing Spectra - An Initial Investigation

Since the Anaspec 36 instrument could not record spectra below shifts of 200cm^{-1} from the exciting line, the Coderg instrument was used in an initial investigative scan. The spectra obtained were used to indicate the positions of bands above shifts of 200cm^{-1} which were subsequently monitored using the Anaspec 36. The bands detected in the Raman spectra of all phases using the Coderg are given in Table 12. A static system was recorded for each phase and then the liquid crystal was made to flow under 30 psi gas pressure.

It can be seen from Table 12 that many similar bands are present in the spectrum of each phase, however distinct differences do occur. Each static phase has a distinct spectrum below 400, however these peaks were not detectable in the flowing material. The exact reason for this is unclear. The region below 400cm^{-1} was therefore of little use in subsequent work.

In the spectrum above 400cm^{-1} , slight shifts were detected between phases in the 407, 1180, 1285 and 1606 bands, therefore these peaks were used in subsequent work on the Anaspec 36.

The major difference seen between the spectra of the different liquid crystal phases recorded using the Coderg instrument, was the shape of the 406 band. This peak was a singlet in the crystalline phase, became slightly distorted in the flowing smectic phase and developed a distinct shoulder (at 436.8cm^{-1}) in the flowing nematic phase. At this stage it is not possible to offer a conclusive explanation for these results, but the shift may well be due to orientation and the subsequent changes in the vibrational environment experienced by the molecules, as will be discussed later.

N.B All wavenumber values quoted in this work are actually the wavenumber shifts from the exciting line.

Table 12 Spectral Peaks seen in the Liquid Crystal Using the Coderg

| Phase | Static | Flowing (at 30 psi) | Comments |
|-------------|--|--------------------------------------|--|
| Crystalline | 140 185 407 636 777.7 812/830 II79/II86 1285 1607 | N/A | Very weak II86 is a shoulder |
| Smectic | 78 III I77.7 215 406.6 635/650 737.5 813/831 1020 II23 II79/II86 1286 1607.1 | 407.7 II83.7 1606 | Distorted shoulder II86 is a shoulder |
| Nematic | 87 98 158 176 170 300-400 407 637.8 778 810/830 II80 1284 I605.7 | 408.5/436.8 II80 160.5 | Several weak bands 436.8 is a shoulder Doublet |

4.2.2 Static and flowing spectra - recorded using the Anaspec 36

The Anaspec 36 instrument was used to record the spectra of both the static and flowing liquid crystal at different flow rates.

The material was firstly made to flow under 50 psi gas pressure, therefore increasing the shear rate over that used on the Coderg, in the hope of producing more pronounced flow alignment of the molecules. Figure 11 illustrates the spectra obtained for the Smectic phase in the lower region, and effects of scatter are very apparent and result in the poor spectrum of the flowing sample. All subsequent work concentrated upon the region above 900 cm⁻¹.

Figure 12 illustrates the static and flowing spectra obtained for all four phases of the liquid crystal, between 900 and 1736 cm⁻¹, and Table 13 lists the wavenumber shifts of the bands present in each phase.

It can be seen from table 13, that the differences observed between the static spectra of different phases are very small. There is a slight shift in the 1243-1245 band, and the 1433-1436 band, of the order of 2-3 wavenumbers and the 1189 band also shows slight variations between phases. The most apparent difference between the static and flowing spectra at 50 psi is the shift and splitting of the 1189 and 1289 peaks in the smectic and nematic phases and the splitting of the 1608 cm⁻¹ band in the smectic phase. However these differences are not easily seen, and spectral subtractions would make the evaluation of any shifts easier.

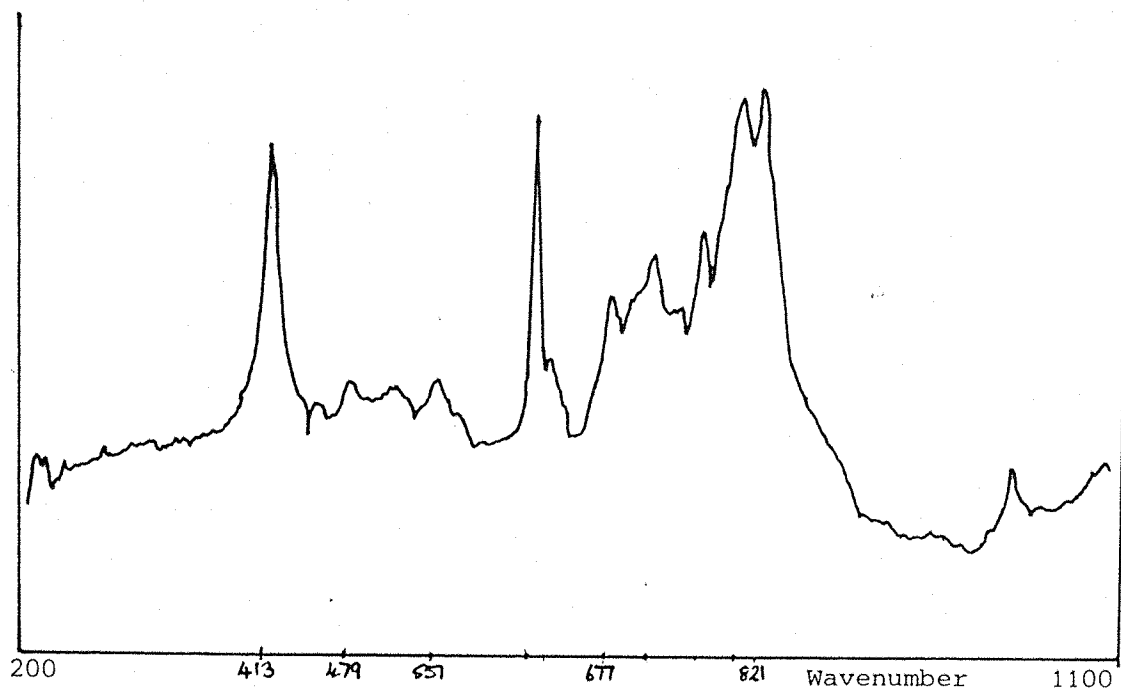
4.2.3 Spectral Subtractions

In order to highlight the differences between the spectra obtained for each static and flowing phase, spectral subtractions were used. Subtractions were done by normalising one band, that is making the intensity the same in the two spectra to be subtracted. This was done by multiplying the less intense spectrum by a correction factor.

Figure 11

Flowing and Static Smectic phase spectra (200-1100 cm^{-1})

1. Smectic static at 25°C



2. Smectic flowing at 30 psi

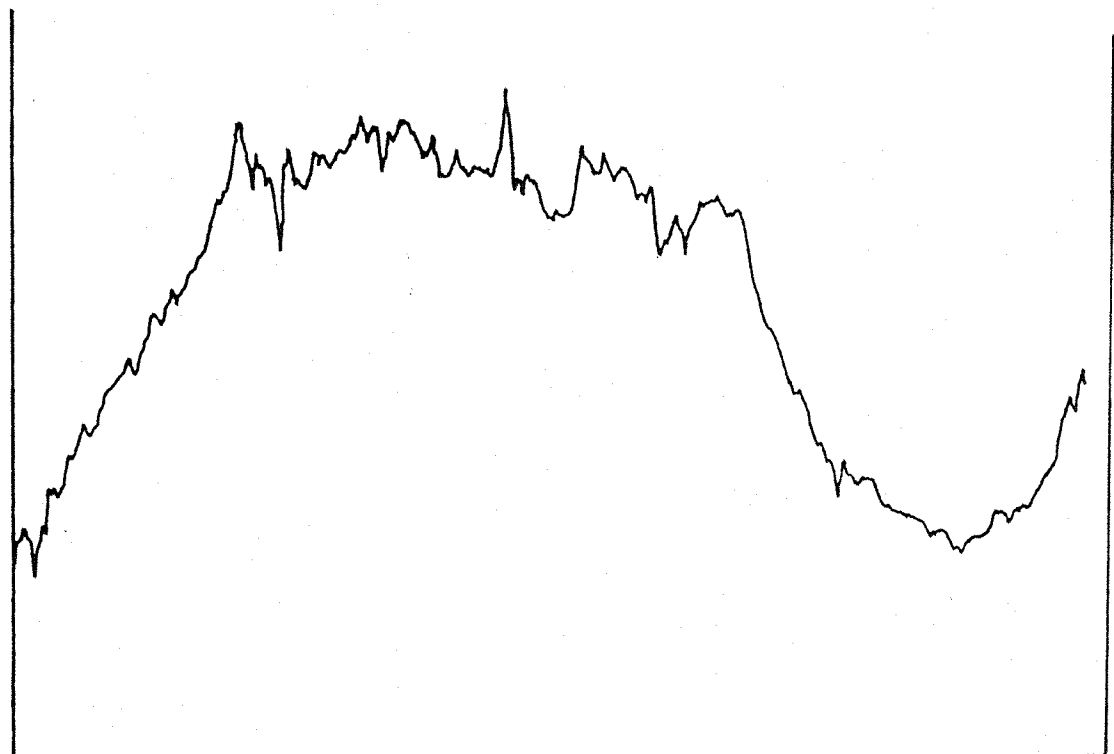


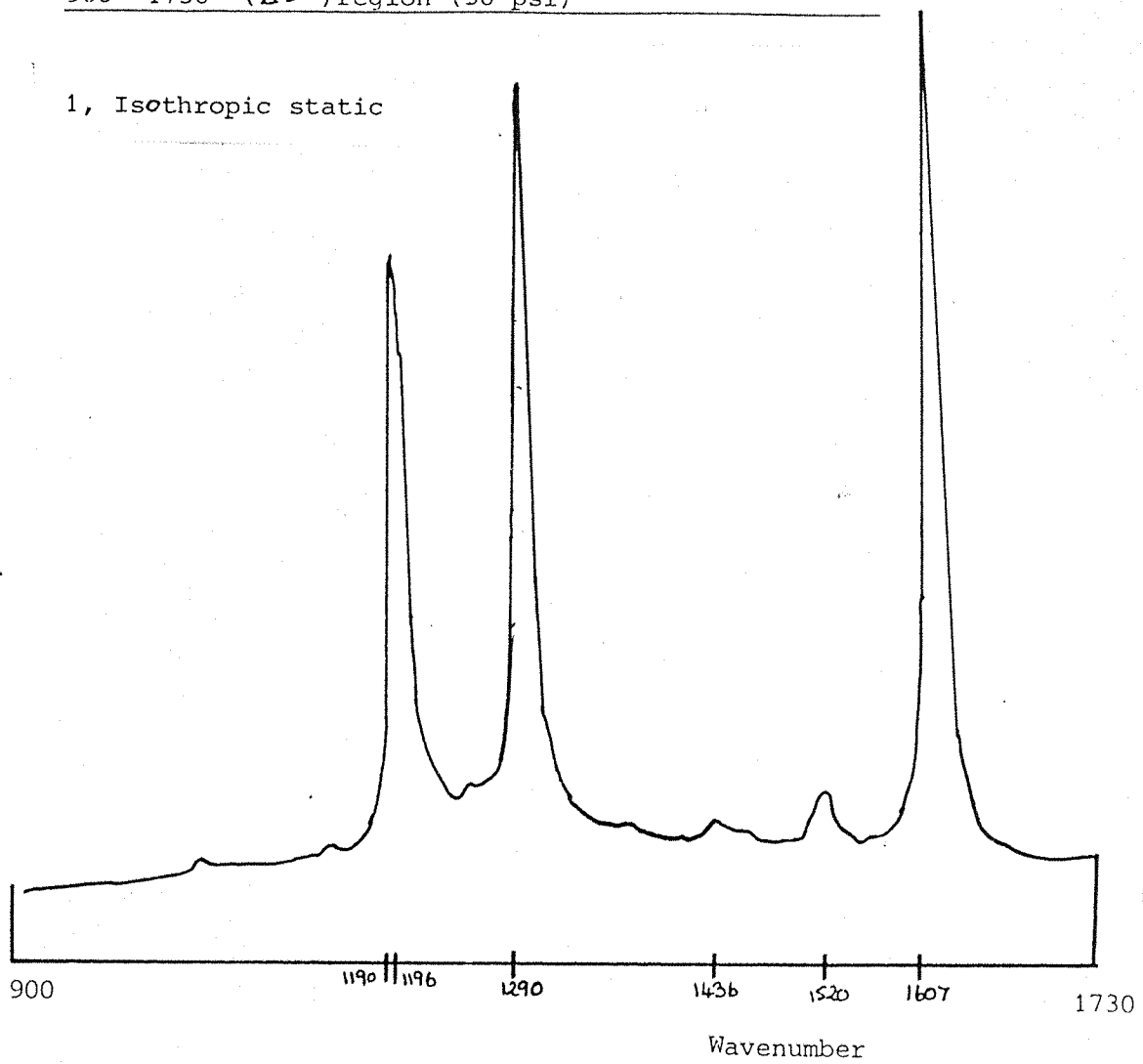
Table 13 Wavenumber shifts in K24, static and flowing, at 50 psi,
between 900 and 1736 cm⁻¹

| Phase | Wavenumber Shift | |
|-------------|------------------|----------------|
| | Static | Flowing |
| Crystalline | II89/II91 | |
| | 1245 | |
| | 1289 | |
| | 1433 | |
| | 1520 | |
| | 1608 | |
| Smectic | II89/II91 | II91/II96 |
| | 1243 | |
| | 1289 | 1289/1291 |
| | 1433 | |
| | 1521 | 1521 |
| | 1608 | 1608/1610 |
| Nematic | II89/II96 | II91/II96 |
| | 1245 | 1243 |
| | 1289 | 1289/1291 |
| | 1434 | |
| | 1520 | 1521 |
| | 1608 | 1608 |
| Isotropic | II89/II91/II96 | II89/II91/II96 |
| | 1244 | 1243 |
| | 1289/1291 | 1291 |
| | 1436 | |
| | 1521 | 1520 |
| | 1607 | 1608 |

Figure 12

Spectra of static and flowing liquid crystal in the
900 -1750 (cm⁻¹) region (50 psi)

1, Isotropic static



2, Isotropic flowing

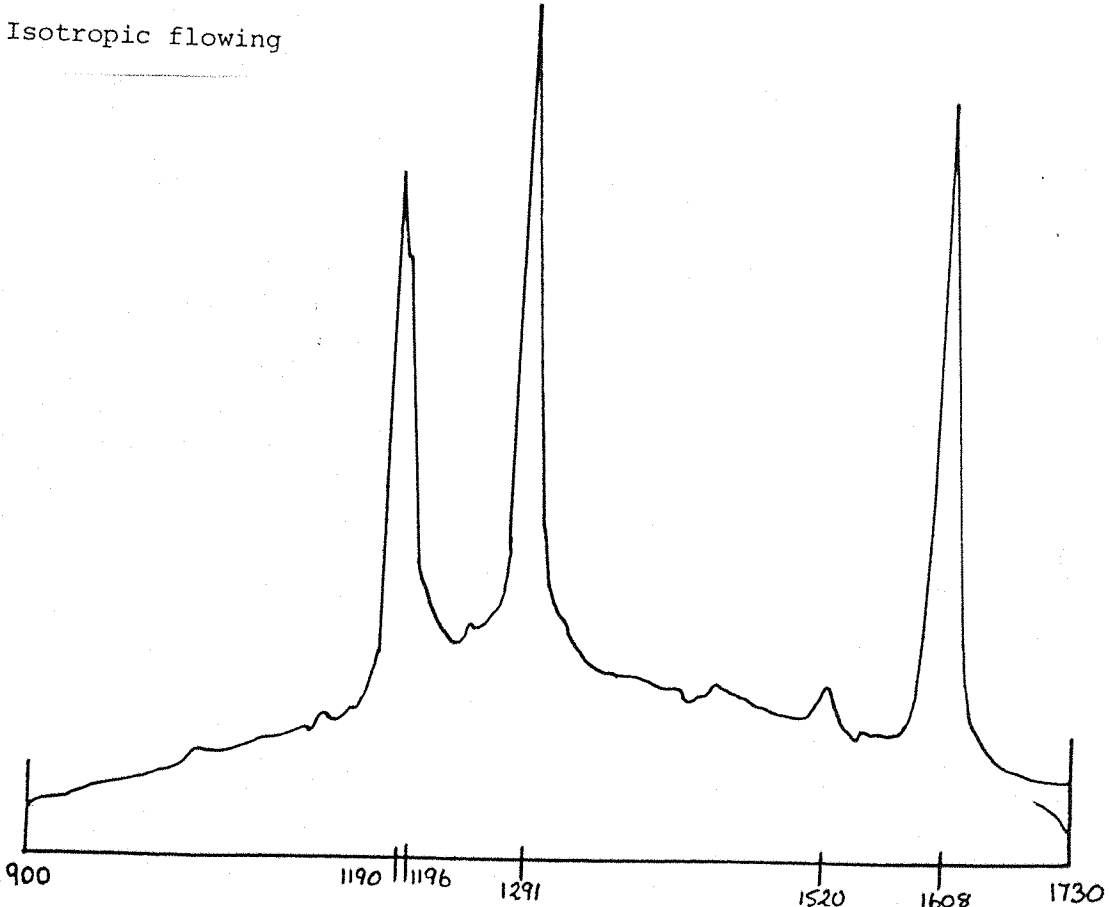


Figure 12 (continued)

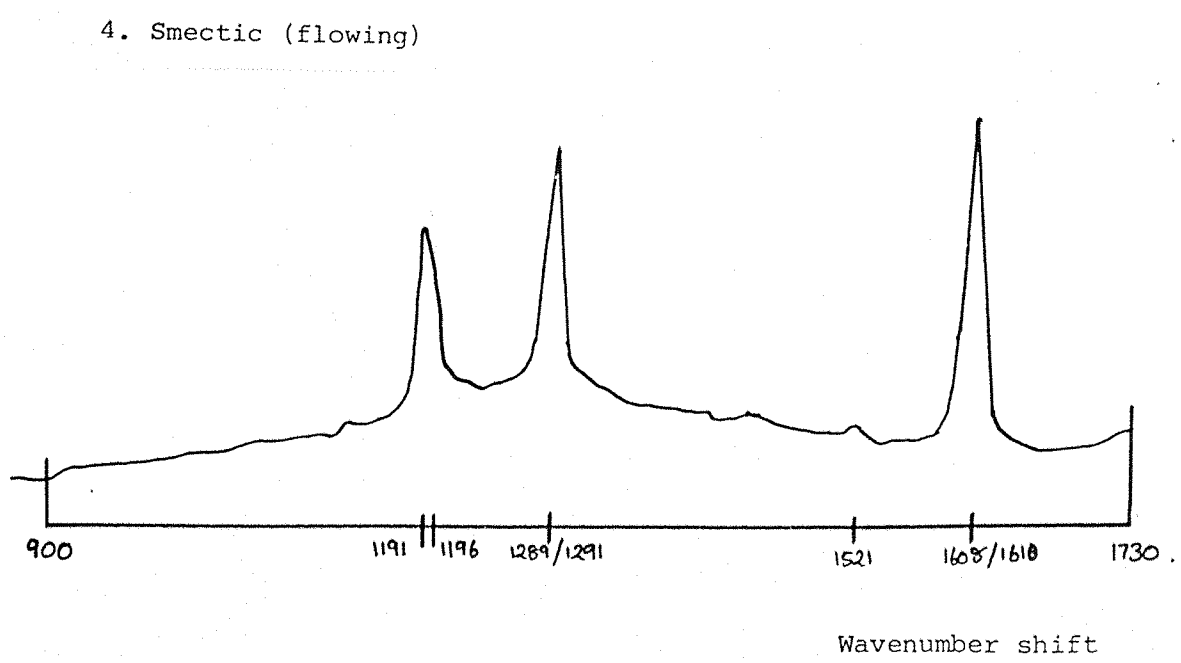
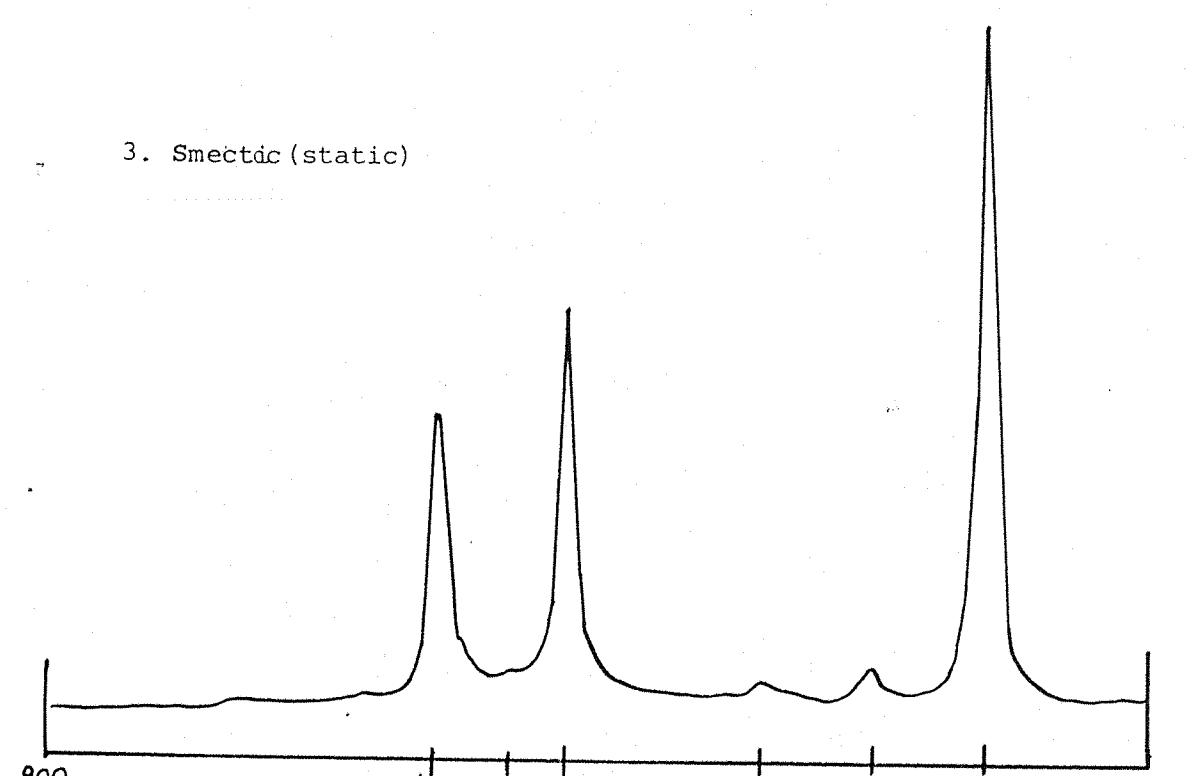
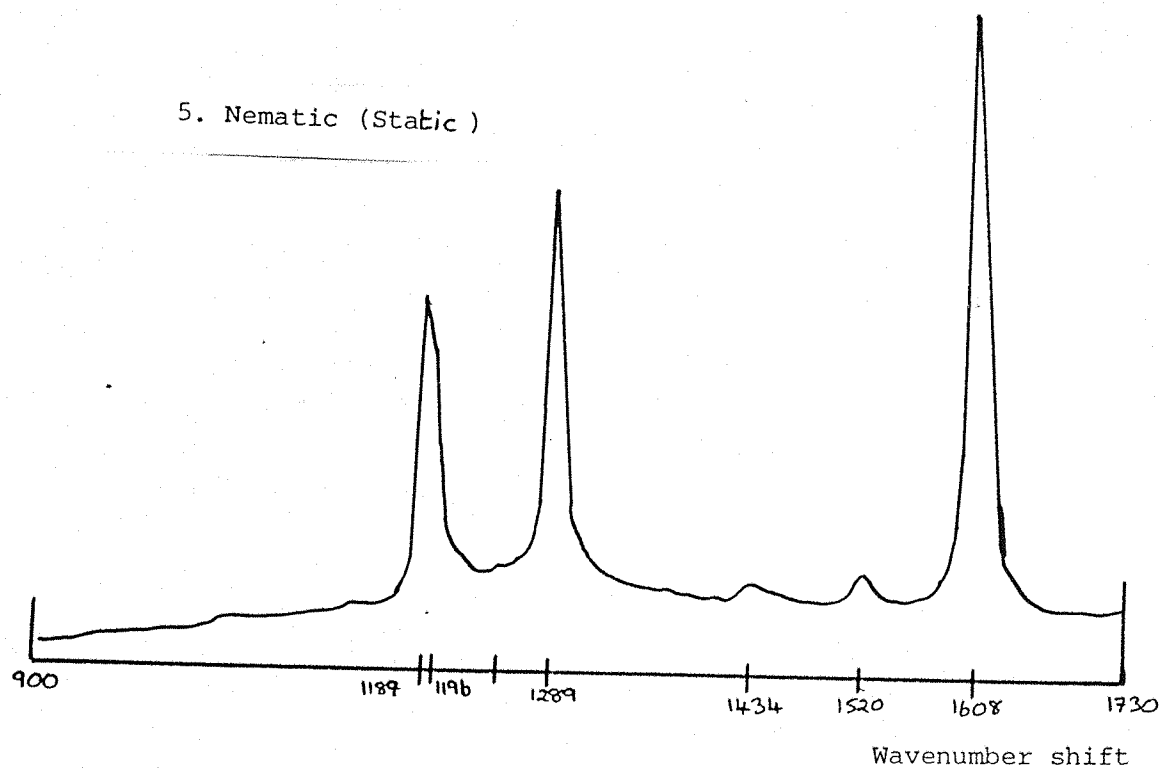
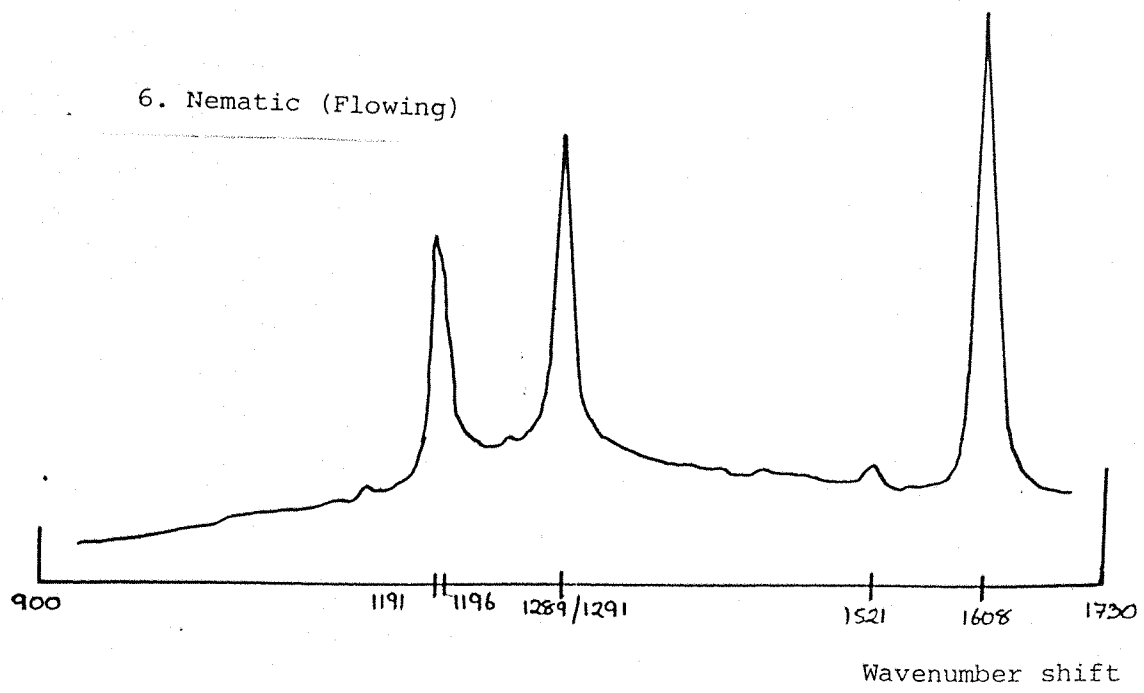


Figure 12 (continued)

5. Nematic (Static)



6. Nematic (Flowing)



The 1600, 1300 or 2200 band was normalised, since these regions had the flattest base lines making subtraction much easier. In each case the flowing spectrum was taken from the static. In the results given a positive peak indicates a stronger band in the flowing spectrum, and a negative band would be due to a more intense band in the static spectrum. Differential peaks indicate that the band was present in both the static and flowing material but had undergone a shift in position. Spectral subtractions were carried out on the results obtained from K 24 flowing under pressures of 30, 50 and 100 psi.

Due to the intense Rayleigh scattering experienced in the lower spectral region, ($200-1100\text{ cm}^{-1}$) particularly with the flowing liquid crystal, it was not possible to do spectral subtractions between the static and flowing spectra in order to pinpoint any major band shifts.

Unfortunately one of the major drawbacks of the Anaspec 36 was that it was unable to plot expanded spectra. Therefore the small details, such as band splitting visible on the VDU, using scale expansion facilities, are often lost. The machine always plotted out the whole spectrum to a standard A4 size. On the spectra used to illustrate this work, where band splitting was observed, with scale expansion, both of the appropriate wavenumber values are given, however the splitting may not always be readily seen on the plots given as they are without expansion.

i) Liquid crystal flowing under 30 psi pressure

Spectral subtractions of the static and flowing liquid crystal, at 30 psi, highlight the differences between the static and flowing spectra for each phase, and the differences between the smectic and nematic states. (Table 14, Fig 13)

The smectic phase exhibits shifts in the 1280 and 2220 bands when flowing, and the nematic phases exhibits shifts in the 1300, 1600 and 2200 bands.

Table 14. Peaks Present in Subtracted Spectra (30 psi)

| Phase | Wavenumber |
|---------|------------|
| Smectic | 1164 |
| | 1281/1309 |
| | 1609 |
| | 2177 |
| | 2226/2233 |
| Nematic | 1335/1323 |
| | 1600/1609 |
| | 2234/2226 |
| | 2181 |

Figure 13

Special subtractions with liquid crystal flowing at 30 psi

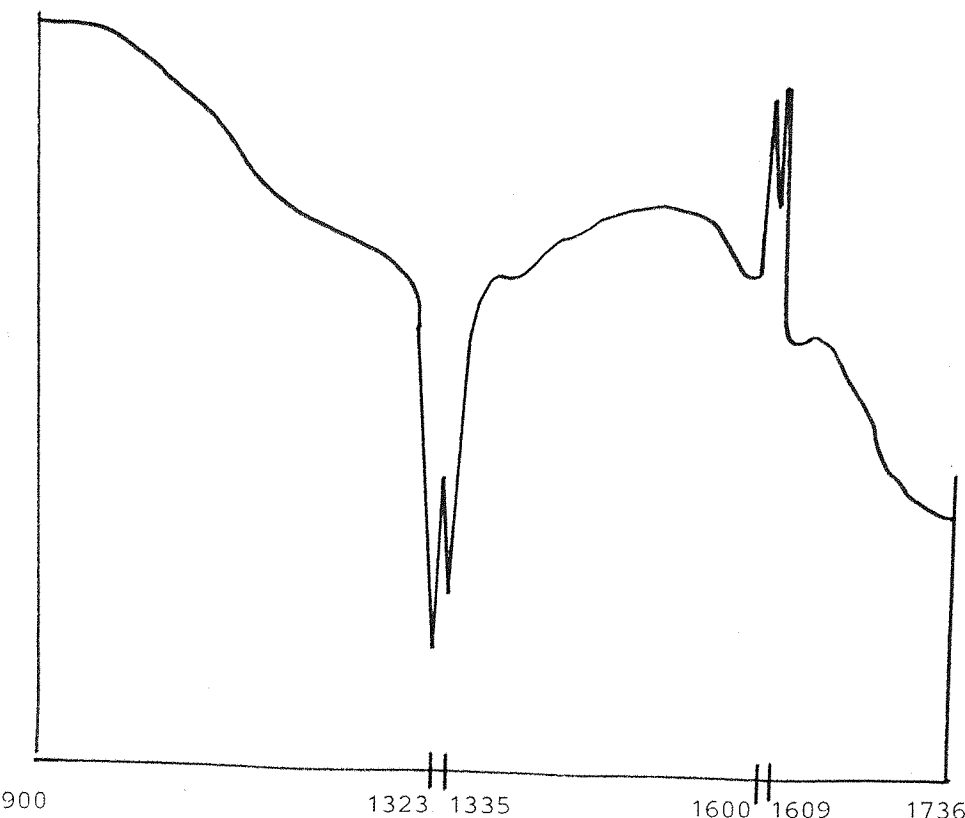
(N.B. These spectra were a little noisy and therefore have been smoothed to produce the following results)

a) 900 - 1736 region

1) SMECTIC (flowing-static)

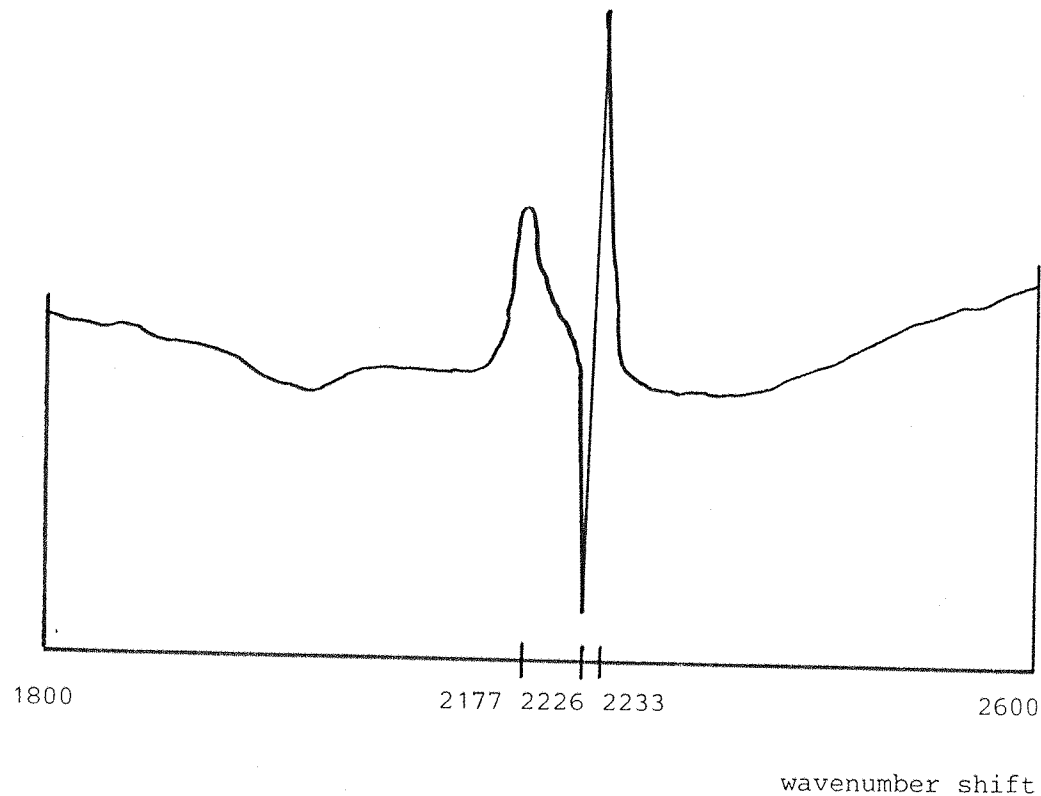


2) NEMATIC (flowing-static)

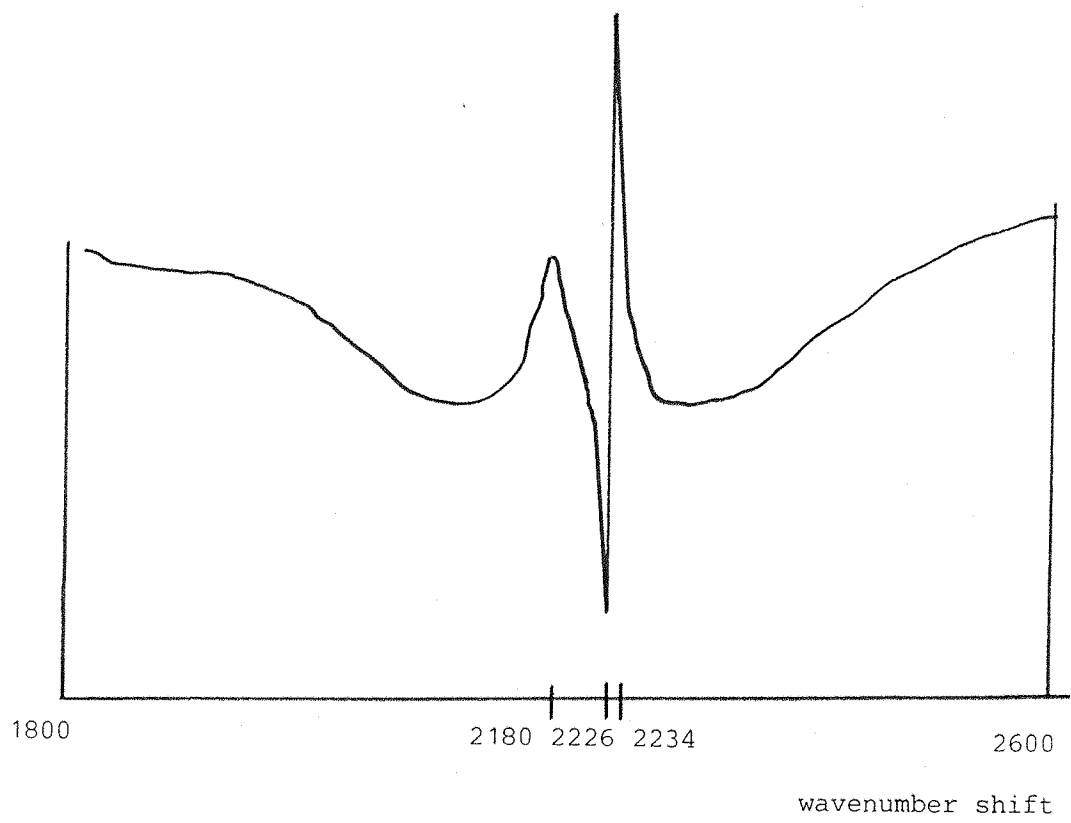


b) 1800 - 2600 region

1) SNECTIC (flowing-static)



2) NEMATIC (flowing-static)



When the 30 psi flowing spectrum was recorded actually at the smectic/nematic transition point, and the result subtracted from the static nematic spectrum, it can be seen that a peak at 1324 cm^{-1} is the only readily detectable peak remaining. This indicates that the spectrum at the transition point resembles that of the nematic static material very closely, since all of the other peaks have been subtracted out. The band at 1324 cm^{-1} is therefore the only difference between the two spectra, the exact origin of this band is unclear. Figure 14 shows the above mentioned subtracted spectrum.

b) Liquid Crystal Flowing under 50 psi Pressure

Subtractions of the static and flowing material at 50 psi, illustrated that all phases, smectic, nematic and isotropic exhibited a shift in the 1600 band. This shift was quite pronounced (more so than at 30 psi) If the spectral subtractions in figure 15 are compared to the original spectra in figure 11, it is quite clear that spectral subtraction provides evidence of shifts not always detectable by eye from separate spectra.

In addition to shifts of the 1600 band, the nematic phase showed a shift in the 1280 peak, and all phases also showed distinct variations in the shifts and resulting shapes of the 1180-1190 band. Table 15 gives the peaks present in all subtractions of spectra obtained at 50 psi flow pressure.

Figure 14

Subtracted spectrum of material at Smectic/Nematic transition from static Nematic material

(Material at transition point flowing under 30 psi pressure)

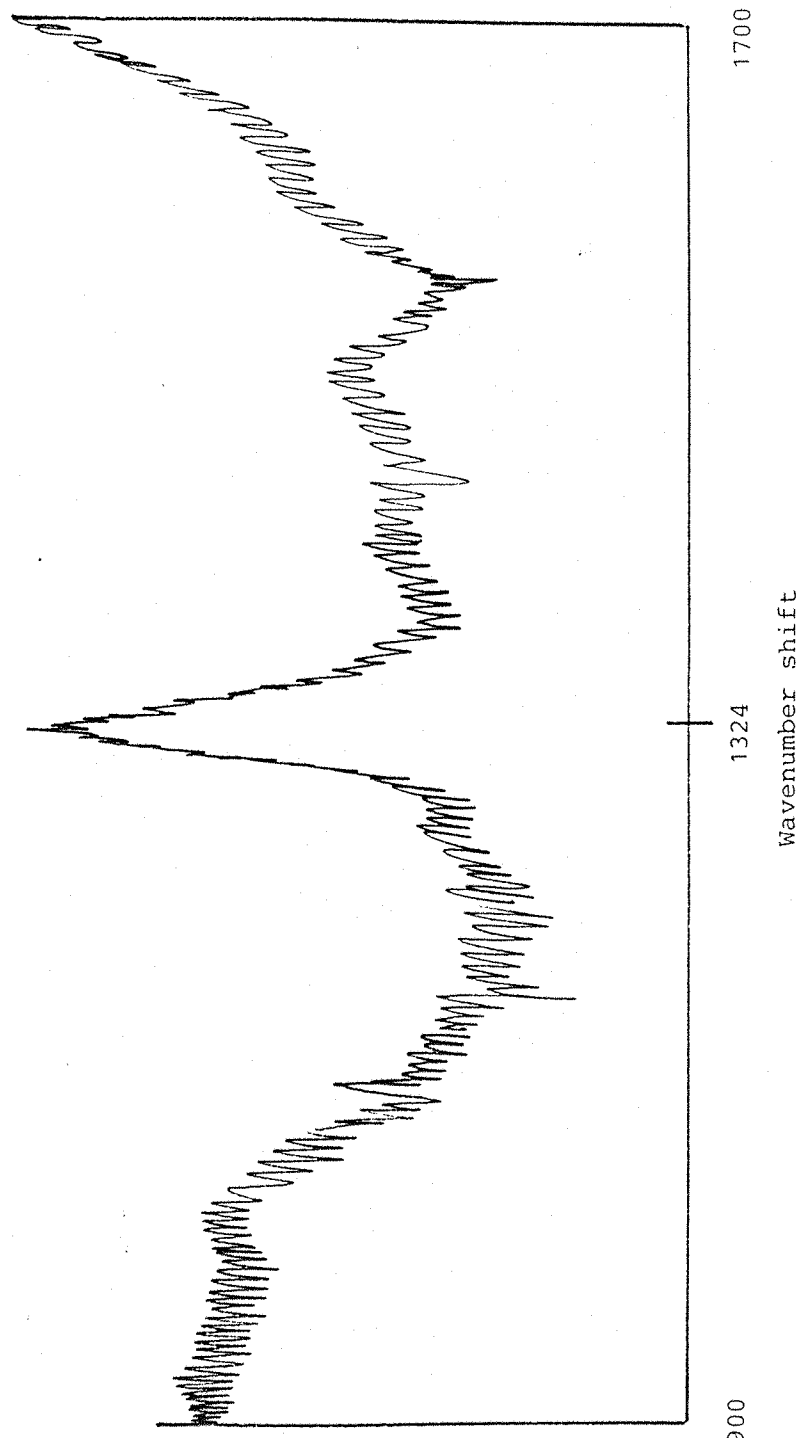


Table 15 Peaks Present in Subtracted Spectra, (50 psi)

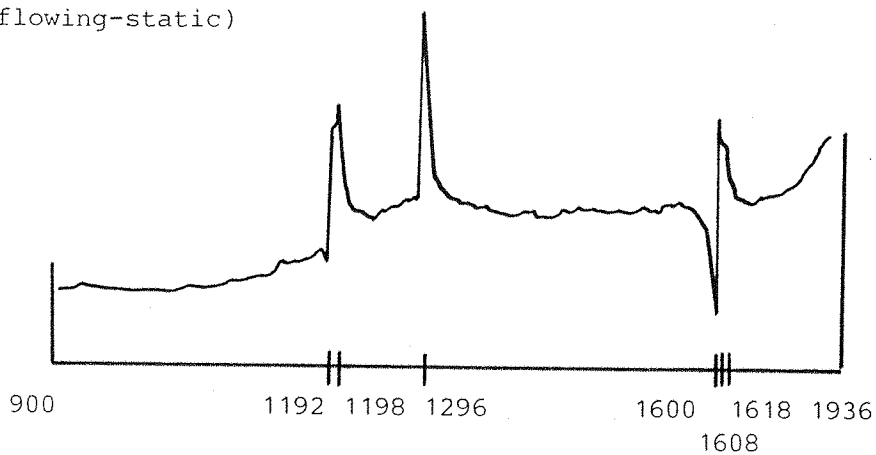
| Phase | Wavenumber |
|-----------|--|
| Smectic | II92/II98 1296 I600/I608.7/I617.7 2245/2237 2188 |
| Nematic | II86/II95/II98 1280/1289.9 I598.8/I605.8/I618 |
| Isotropic | II86/II91/II98 1292 1607.7/I611/1616 |

Figure 15

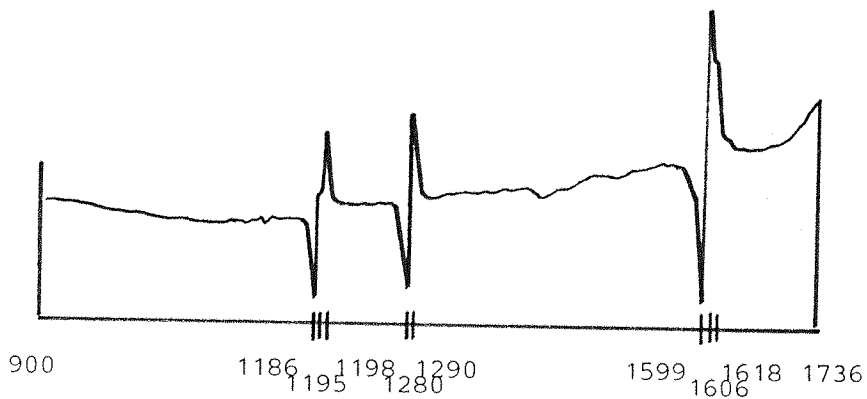
Spectral subtractions with liquid crystal flowing at 50 psi

(all subtractions not normalised wrt 1600 band)

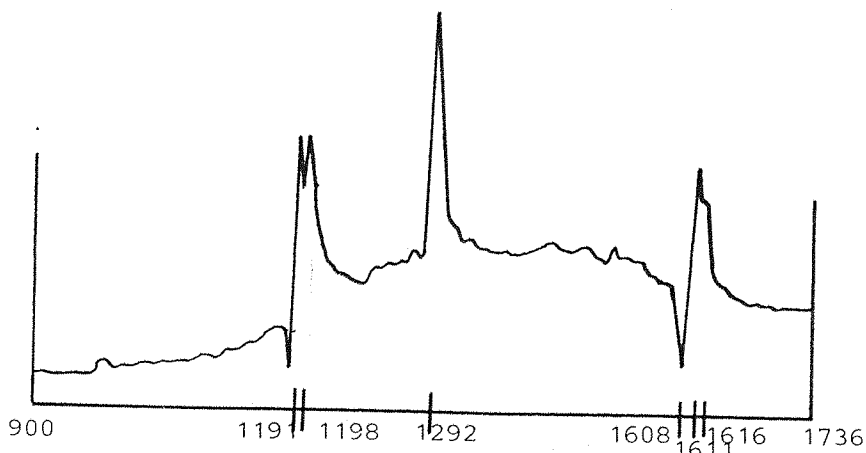
1) SMECTIC (flowing-static)



2) NEMATIC (flowing-static)



3) ISOTROPIC (flowing-static)



c) 100 psi

When the liquid crystal was made to flow under 100 psi pressure the smectic phase exhibited shifts in the 1300 and 2230 bands, whilst the nematic had shifts in the 1200, 1300 and 2230 bands, as illustrated in Figure 16 and Table 17. The major differences between the smectic and nematic subtractions here are the splitting of the 1200 band in the nematic phase, which is not so pronounced in the smectic, and the shift of the 2190 smectic band to 2193 in the nematic spectrum.

Table 17 Peaks Present in the Subtracted Spectra, (100 psi)

| Phase | Wavenumber |
|---------|----------------|
| Smectic | 1202 |
| | 1302/1310 |
| | 1621 |
| | 2190 |
| | 2239/2247 |
| | 2427 |
| Nematic | 1201/1213/1222 |
| | 1300/1309 |
| | 1621 |
| | 2193 |
| | 2239/2247 |
| | 2427 |

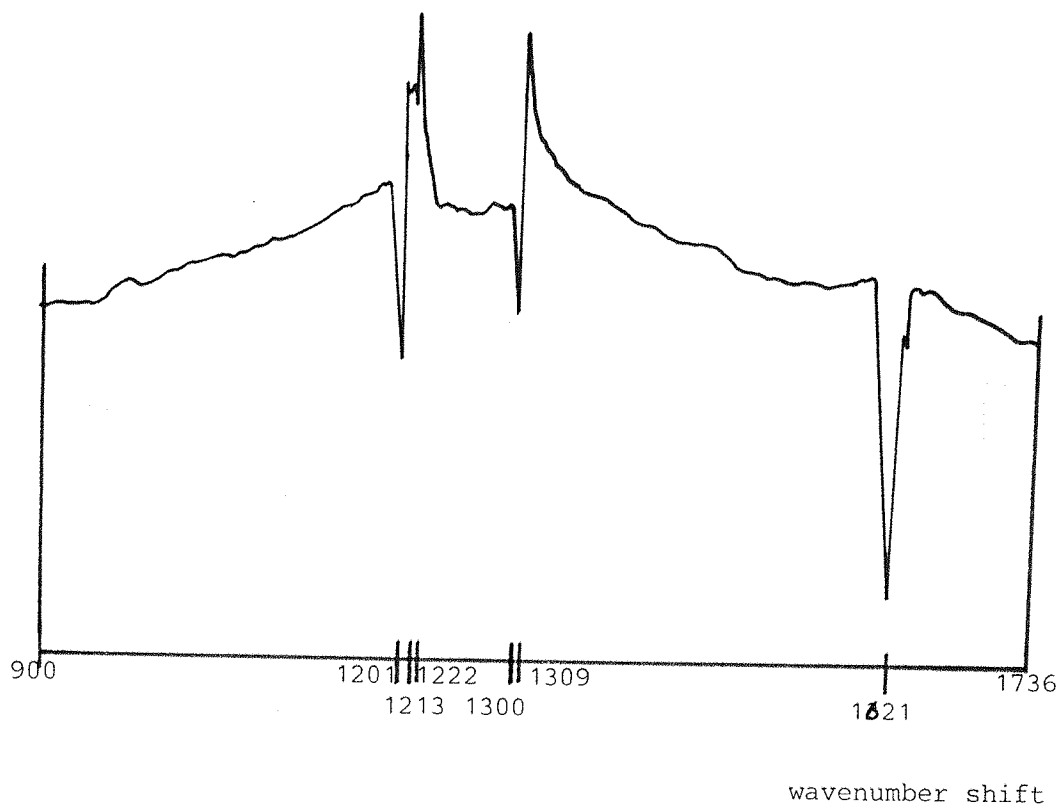
4.2.4 Comparison of subtracted spectra of each phase, at different flow rates

Having compared the results of flowing and static material, and the differences between each phase, both static and flowing, with spectral subtractions, the final point to be

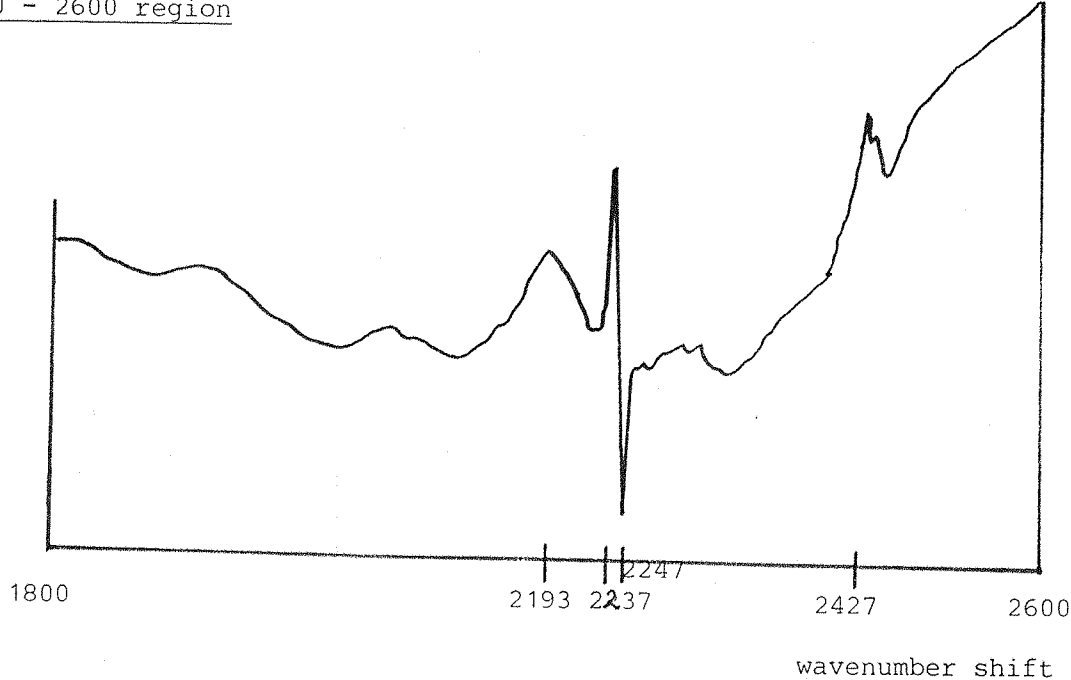
Figure 16

Spectral subtractions with liquid crystal flowing at 100 psi in Nematic phase
(smoothed spectra)

1) 900 - 1736 region



2) 1800 - 2600 region



discussed is whether each phase has a tendency to exhibit different characteristics at different flow rates. Since the smectic and nematic phases are the truly liquid crystalline phases present they will be discussed here. It can be seen by comparing Tables 15, 16 and 17, for the smectic phase, that all of the peaks present undergo an overall shift to higher wavenumbers as the flow rate increases, as illustrated below.

Table 18 Smectic peak shifts with increasing flow rate

| 30 psi | 50 psi | 100 psi |
|--------|---------------|---------|
| 1164 | 1192/1197.9 | 1202 |
| 1281 | 1296.3 | 1302 |
| 1609 | 1608.7/1617.7 | 1621 |

For the nematic phase the 1180, 1280 and 1600 bands again show a distinct shift to higher wavenumbers, with increasing flow rate; as shown in the table below.

Table 19 Nematic peak Shifts with increasing flow rate

| 30 psi | 50 psi | 100 psi |
|-------------|---|------------------------------------|
| 1600 - 1609 | 1186 - 1198 1280 - 1290 1599 - 1618 | 1201 - 1222 1300 - 1309 1621 |

Previous work by Vettegren (40) upon overstressed bonds in polymeric materials, has shown that, a shift to higher wavenumbers in the infra-red spectrum is indicative of bondstress. If this theory is expanded it would not seem unreasonable to propose that the band shifts seen in the liquid crystal phases at higher flow rates would be due to a similar phenomenon, resulting from shear flow alignment, exerting stresses on molecular bonds. However this has not yet been confirmed, and further work is currently underway.

CHAPTER 5

CONCLUSIONS

The work reported in the proceeding sections was carried out over a period of one academic year, prior to employment in the polymer industry. The research work carried out by the polymer group at Southampton covers a variety of topics related to the correlation of molecular structure and properties of polymeric substances, and the two areas of work reported here are considered to be of current general interest to the polymer industry as a whole.

5.1 Chain Rupture during deformation of polymeric samples

Considerable work over several years has given rise to the current theories regarding the structure and detailed morphology of solid polyethylene. Recently work has concentrated upon relating early structural studies with the results obtained from studying the effects of the thermal history of the sample on the morphology of solid polymer, and the structures present in deformed materials e.g. plastically deformed polyethylene. The principle aim of the work at Southampton was to attempt to say something about the structure of a solid polymer and the changes that occur when stress is applied. One member of the group, Mr. M. Taylor, has been investigating the structural changes that occur when polyethylene is deformed to between 2 and 10 times its starting dimensions, and in a complementary line of research it was observed that weak infra-red absorptions occurred in polyethylene as a result of its deformation. It was presumed that these were related to bond rupture, that is, that they might be correlated with results already in the literature on bond rupture during deformation. The results reported in Chapter 3 are an attempt to quantify and explain this phenomenon.

The results show that:-

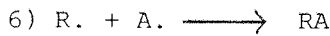
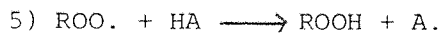
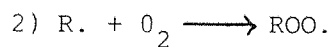
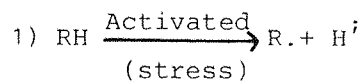
- 1) The increase in new group formation is inversely proportioned to the original sample thickness.
- 2 The formation of carbonyl groups in a deformed sample only occurs if atmospheric oxygen is available, whereas an increase in the terminal vinyl unsaturation is seen in samples drawn in either oxygen or nitrogen.
- 3) The increase in new end groups is related to the extent of drawing to which the sample is subjected.
- 4) After deformation the increase in new groups may take up to 96 hours to reach a stable maximum value.
- 5) The increase seen in new groups with deformation, decreases as the temperatures at which drawing was carried out increases.
- 6) Small increases in carbonyl absorptions have been detected in samples subjected to loading prior to deformation.

From the proceeding results it may be concluded that:-

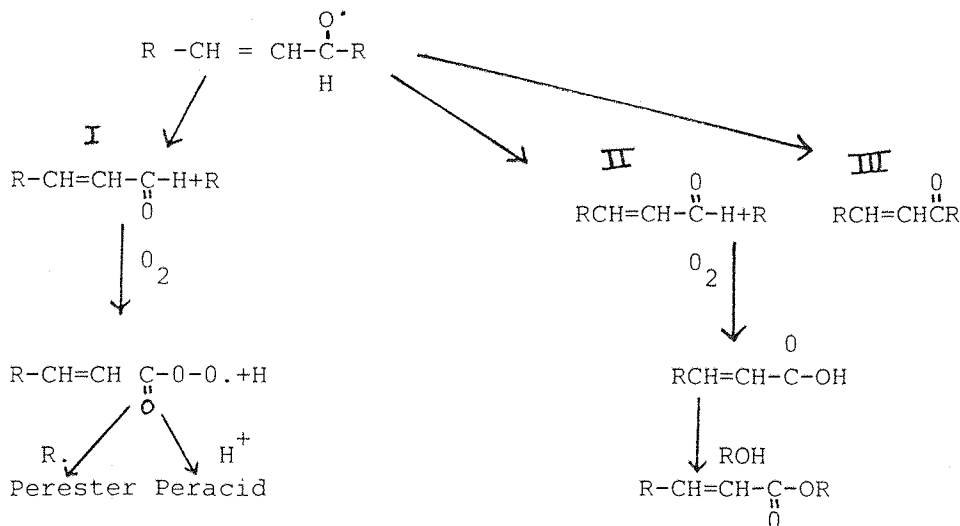
- 1) The increases seen in the infra-red bands may be associated with bond rupture. This association is indirect in that it is based upon the results obtained from a series of tests.
- 2) The smaller increases seen in new end groups for thicker samples implies that this is a surface effect, supporting the proposal by Vettegren⁽⁴⁴⁾ that a higher concentration of overstressed bonds exists at the surface of the sample, leading to more chain breakages at the film surface.

3) The increases seen in carbonyl content and terminal vinyl unsaturation depending upon the atmosphere of drawing indicates that there is some competition between the two reactions and that the relative amounts of each produced will depend upon the availability of atmospheric oxygen.

4) The continuing increase in end group concentration detected up to 96 hours after deformation implies that some type of chain reaction is initiated by the initial chain ruptures, which will continue after the stress in the sample has been released. Such a chain reaction has been proposed by Ward and Luongo, as long ago as 1961 (33). Some of the possible steps are as follows:-



From (4)



- 5) As the temperature at which deformation is carried out increases the polymer chains gain thermal energy and are therefore more mobile and able to reorient themselves more easily upon the application of a load. Therefore the number of chains broken decreases, culminating in fewer new end groups.
- 6) Assuming the transferability of extinction co-efficients between like samples [a very bold and largely unfounded assumption] it is shown that for a specimen deformed to three times its original length up to 7×10^{19} rupture/cm³ may occur.

To date the most widely accepted method of assessing the number of bonds ruptured when a polymer is manipulated is E.S.R.. Measurements using this technique for materials such as polyethylene or polypropylene are almost always done after the sample has been broken at low temperatures, and no attempt is made to manipulate the sample at ambient temperatures because of the highly reactive radicals formed. As a result of this experimental difficulty bond rupture in interesting environments cannot be studied. The method described in this work is applicable at all temperatures in all environments, and in principle at all strain rates. The limitation of infra red (and this may be severe) is that of sample thickness, for the transmission technique reported here.

As stated the quantitative analysis of the carbonyl absorptions has shown that up to 7×10^{19} new carbonyl groups may be formed upon deformation of a sample to a draw ratio of 3. If we make due allowance for the errors involved in transferring the extinction coefficient, the precise value will lie between 10^{18} and 10^{20} rupture/cm³. Assuming the oriented sample to be homogenous and perfectly oriented the number of C-C bond per cm³ for polyethylene is of the order of 10^{21} therefore the proportion of available bonds actually broken is of the order 1 - 10%

Peterlin was aware of the small number of chain ruptures occurring during deformation and exploited this fact when forming his theory of plastic deformation, in which he states that lamella slip rotation and alignment are the major processes active during drawing, with little mention of any bond rupture. At present there is considerable interest in the melting theory proposed by Harrison, however the low value of bond rupture reported here takes us no further towards a solution of the processes active during polymeric deformation, except to say that either theory proposed by Peterlin or Harrison would be acceptable, since they both propose low values for chain rupture.

5.2. Shear Flow Induced Alignment

There has been a continuing interest in the structure and general properties of flowing polymer melts. Attempts have therefore been made at Southampton to study a flowing polymer melt using Raman spectroscopy and x-ray diffraction measurements. As a parallel to this work and in view of the interest in the polymer world in liquid crystal forming polymers an experiment was devised and constructed to study the effect of shear on a liquid crystal.

It was observed that:-

- 1) An experiment could be made to work and constructed to fit within the sample area of a Raman spectrometer.

- 2) Shifting occurred in the bands at high shears, presumably due to changes in the detail of the vibrational behaviour.

The shifting of bands can be explained by either very high pressures, temperature or structural changes. Since the pressures involved here were too low and the temperature was kept constant the shifting must be indicative of structural changes. These structural changes could be of two sorts, that is, due to orientation or the development of order.

Evidence for the development of order is weak, but certainly not procluded, and it has therefore been assumed that orientation occurs and that this explains the observed effects.

It is clear that in the future several developments need to be made within the apparatus and that the system should be studied by alternative techniques, such as, infra-red spectroscopy and x-ray diffraction. These techniques will give further evidence of orientation or order.

REFERENCES

- 1) Brydson, Plastics Materials - Butterworths 1975
- 2) P.J. Cutler, Optical Multichannel Laser Raman Spectroscopy - International Laboratory June 1983
- 3) S. Chandrasekhar & N.V. Madhusudana, Liquid Crystals 3, Pt.1, p.251-262 -Gordon & Breach 1970
- 4) K. Kobayashi, Liquid Crystals 3, Pt.II, p.925-936 - Gordon & Breach 1970
- 5) W. Helfrich, Three Dimensional Classification of Liquid Crystals *
- 6) J. Prost & N.A. Clark, Hydrodynamic Properties of Two Dimensionally Ordered Liquid Crystals *
- 7) L. Lei, Critical Properties of Neumatic-Isotopic Transition in Liquid Crystals *
- 8) J. Bulkin & F.T. Prochaska, J.C.P. 54 Number 2 15.1.71
- 9) S.N. Prasad & S. Venugopalan, Orientational Statistics in 80LB - Raman & IR Study
- 10) B. Bulkin & W. Lok, SPC. 77 1973 326
- 11) Liquid Crystals, G. Bromm, F. Dienes, M. Labes, Proceedings of the International Conference on Liquid Crystals - Kent State University August 1965 - Gordon & Breach science publishers
- 12) Liquid Crystals 3, Pt.II, G. Brown & M. Labes - Gordon & Breach 1970
- 13) Liquid Crystals and Ordered Fluids - Proceedings of an American Chemical Society Sy;mpoium on Ordered Fluids and Liquid Crystals - NUYC September 1969 - J. Johnson & R. Porter, Penium Press 1970
- 14) Meier, Sackmann, Grabmaier - Applications of Liquid Crystals, Springer Verlag NY 1975
- 15) C. Gahwiller - Physical review letters 28 No.24 1972
- 16) Liquid Crystals CH3 - Lecture notes
- 17) J. M. Andrews, I.M. Ward JMS 5 1970 411-417

18) A. Keller, D.P. Pope JMS 6 1971 453-478

19) A. Peterlin JMS 6 1971 490-508

20) D. Aitken, D.J. Cutler Polymer 20 1979

21) P.J. Flory, D.Y. Yarn Nature 272 March 1978

22) A. Keller - Crystalline Polymers; an introduction 1979 146-166

23) T. Yoshida, Y. Fugiwara - Polymer 24 1983

24) R. Cornelius, A. Peterlin - Die Makromole Kulart Chemie 103 1967 193-203

25) G. Capaccio, I.M. WARD - Polymer 15 1974

26) T.M. Stoekel, J. Blasius JPS Polymer Physics 16 1978 485-500

27) M. Sakaguchi, J. Sohma JPS Polymer Physics 13 1975 1233-1245

28) M. Sakaguchi, J. Sohma - Reports on progress in polymer physics in Japan 16 1973

29) K.L. Derries, R.H. Smith, B.M. Fanconi - Polymer 21 1980

30) D.K. Roylance, K.L. Derries - Polymer preprints 17 No.2 1976 720-725

31) D.K. Roylance - Applications in Polymer Spectroscopy Symposium, San Francisco - Edited by E.G. Brame 1979

32) K.L. Deiries - Polymer preprints 17 No.1 1976 100-105

33) D.L. Wood, J.P. Luongo - Modern Plastics March 1961

34) S.N. Zhurkor, V.E. Karsukov JPS Poly Physed 12 1974 385-398

35) K.L. Deiries JA.P.S. Applied polymer symposium 1979 439-453

36) T. Kawashima, S. Shimada, H. Kashiwabara, J. Sohma - Polymer 5 1973 135

37) M.L. Wiliams & K.L. Deiries - Surfaces and Interfaces, p.139, Syracuse University Press 1968

38) C.T. Graves, M.G. Onnerod - Polymer 43 1963 81

39) A.E. Brotskii - Doklady Akademii, USSR 156 1147 (1967)

40) T.C. Chiang, J.P. Bibilia J.P.S. 10 (1972) 2249

41) V.I. Vettegren, I.I. Novak J.P.S. - Poly. Phys. Ed. 11 1973 2135-2142

42) S.I. Velieu, V.E. Karsukar, V.I. Vettegren - Polymer Mech. 7 (1973) 347

43) S.N. Zhurkar, V.A. Zakrevskyi, V.E. Karsukar, V.S. Kuksenko J.P.S. Part A-2 10 (1972) 1509-1520

44) D.K. Raylance, K.L. Devries J.P.S.(B) 9 (1971)

45) V.I. Vettegren, A.E. Tschmel - European Polymer Journal 12 No.12 (1976) 853-858

46) L.D. Esposito, L. Koenig - Polymer Eng. Sci. 19 No.2 1979 162-165

47) S.I. Velieu, V.E. Karsukov, V.I. Vettegren, I.I. Novak - Polymer Mechanics (USSR) 3 1971 347-350

48) D.L. Wood, J.P. Luengo - Modern Plastics March 1961

49) S.I. Velieu, V.I. Vettegren, I.I. Novak - Polymer Mechanics (USSR) 3 (1970)

50) J.S. Fritz, G.H. Schenk - Quantitative Analytical Chemistry 3rd Edition, Allyn and Bacon Inc. 1974

51) Developments in Polymer Characterisation - 2, J.V. Dawkins, Applied Science Publishers 1980

52) M.Phil Thesis, J. Vile, Southampton University

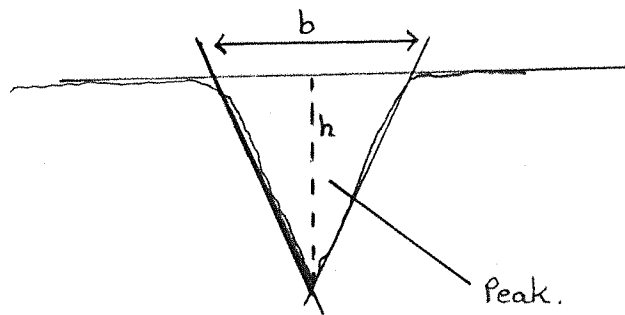
53) J.A. Brydson - Flow Properties of Polymer Melts, Butterworth 1970

* Available from author, exact source unknown

APPENDIX 1.

CALCULATION OF RESULTS

Increases in the carbonyl and vinyl absorbances were calculated as the peak area. The shape of the peak was taken as being triangular and therefore the standard area equation, $\text{Area} = \frac{1}{2} \text{base} \times \text{height}$ was used. A base line was drawn onto the spectrum and measurements taken as shown below:-



$$\text{Area} = \frac{1}{2} b \times h$$

It was possible to measure b and h to an accuracy of 0.5mm on the spectra obtained and each value quoted in the test is an average of between two and six results, obtained from repeating scans on all samples. The reduction in sample thickness due to drawing was also taken into account when calculating results.